

EFFECT OF GOLD NANOPARTICLES ON CYTOCHROME P450 GENE
EXPRESSION IN HEPG2 CELL LINE

Miss Ladear Wangcharoenrung

A Thesis Submitted in Partial Fulfillment of the Requirements
for the Degree of Master of Science Program in Pharmaceutical Technology
Department of Pharmaceutics and Industrial Pharmacy
Faculty of Pharmaceutical Sciences
Chulalongkorn University
Academic Year 2010
Copyright of Chulalongkorn University

ผลของนาโนพาร์ทิเคิลทองคำต่อการแสดงออกของยีนไซโตโครมพี 450 ในเซลล์เฮปจี2

นางสาวลาเตียร์ หวังเจริญรุ่ง

วิทยานิพนธ์นี้เป็นส่วนหนึ่งของการศึกษาตามหลักสูตรปริญญาวิทยาศาสตรมหาบัณฑิต
สาขาวิชาเทคโนโลยีเภสัชกรรม ภาควิชาวิทยาการเภสัชกรรมและเภสัชอุตสาหกรรม

คณะเภสัชศาสตร์ จุฬาลงกรณ์มหาวิทยาลัย

ปีการศึกษา 2553

ลิขสิทธิ์ของจุฬาลงกรณ์มหาวิทยาลัย

Thesis Title EFFECT OF GOLD NANOPARTICLES ON
CYTOCHROME P450 GENE EXPRESSION IN HEPG2
CELL LINE
By Miss Ladear Wangcharoenrung
Field of Study Pharmaceutical Technology
Thesis Advisor Assistant Professor Warangkana Warisnoicharoen, Ph.D.
Thesis Co-Advisor Professor Apiwat Mutirangura, M.D., Ph.D.

Accepted by the Faculty of Pharmaceutical Sciences, Chulalongkorn
University in Partial Fulfillment of the Requirements for the Master's Degree

..... Dean of the Faculty of
.....Pharmaceutical Sciences
(Associate Professor Pintip Pongpech, Ph.D.)

THESIS COMMITTEE

.....Chairman
(Associate Professor Parkpoom Tengamnuay, Ph.D.)

.....Thesis Advisor
(Assistant Professor Warangkana Warisnoicharoen, Ph.D.)

.....Thesis Co-Advisor
(Professor Apiwat Mutirangura, M.D., Ph.D.)

.....Examiner
(Assistant Professor Nontima Vardhanabhuti, Ph.D.)

.....External Examiner
(Plearnpis Luxananil, Ph.D.)

ลาเคียร์ หวังเจริญรุ่ง : ผลของนาโนพาร์ทิเคิลทองคำต่อการแสดงออกของยีนไซโตโครมพี 450 ในเซลล์
เฮปจี2. (EFFECT OF GOLD NANOPARTICLES ON CYTOCHROME P450 GENE EXPRESSION
IN HEPG2 CELL LINE) อ. ที่ปรึกษาวิทยานิพนธ์หลัก : ผศ.ภญ.ดร. วรางคณา วาริสน้อยเจริญ, อ.ที่
ปรึกษาวิทยานิพนธ์ร่วม : ศ.นพ.ดร. อภิวัฒน์ มุทิรากร, 95 หน้า.

ปัจจุบันนาโนพาร์ทิเคิลทองคำถูกนำมาใช้ในทางการแพทย์มากขึ้น เช่น การนำส่งยา การรักษาโรค และ
การวินิจฉัยโรค การสังเคราะห์นาโนพาร์ทิเคิลของทองคำใช้วิธีคักชัน ในการทดลองนี้มีการใช้สารทำให้เสถียร
สองประเภทคือ ซิเตรทและ โพลีเอททิลีนอิมิน และใช้นาโนพาร์ทิเคิลทองคำเพื่อทดสอบการเหนี่ยวนำการ
แสดงออกของยีนไซโตโครมพี450 ของมนุษย์จำนวน 5 ชนิด ได้แก่ CYP1A1, CYP1A2, CYP2C9, CYP2E1 และ
CYP3A4 โดยวิธีเรียลไทม์พีซีอาร์ จากการศึกษาพบว่าขนาดเฉลี่ยของเส้นผ่านศูนย์กลางของอนุภาคนาโนพาร์
ทิเคิลของทองคำที่เตรียมโดยใช้ซิเตรทและ โพลีเอททิลีนอิมินเป็นสารทำให้เสถียรเท่ากับ 15.00 ± 2.77 และ 5.02
 ± 1.81 นาโนเมตร ตามลำดับ ขนาดประจุของนาโนพาร์ทิเคิลของทองคำที่ใช้ซิเตรทและ โพลีเอททิลีนอิมินเป็น
สารทำให้เสถียรวัดได้ดังนี้ -40.60 ± 1.22 และ 8.10 ± 1.59 มิลลิ-โวลต์ตามลำดับ ไม่พบว่านาโนพาร์ทิเคิลของ
ทองคำที่ใช้ซิเตรทเป็นสารทำให้เสถียรมีความเป็นพิษต่อเซลล์เฮปจี2 เมื่อทดสอบที่ความเข้มข้น 90 ไมโครโมลาร์
สำหรับนาโนพาร์ทิเคิลของทองคำที่ใช้โพลีเอททิลีนอิมินเป็นสารทำให้เสถียร พบค่าความเข้มข้นที่ยับยั้งได้ร้อยละ
50 (IC_{50}) เท่ากับ 37.58 ± 1.15 ไมโครโมลาร์ จากการศึกษาผลของนาโนพาร์ทิเคิลทองคำต่อการแสดงออก
ของยีนพบว่า นาโนพาร์ทิเคิลทองคำที่ใช้ซิเตรทเป็นสารทำให้เสถียรที่ความเข้มข้น 10 ไมโครโมลาร์สามารถ
เหนี่ยวนำการแสดงออกของยีนได้อย่างมีนัยสำคัญ ($p \leq 0.05$) ใน CYP1A2 และ CYP2C9 โดยมีค่าการเหนี่ยวนำ
เท่ากับ 2.32 ± 0.35 และ 1.65 ± 0.39 เท่าตามลำดับ ส่วนนาโนพาร์ทิเคิลทองคำที่ใช้โพลีเอททิลีนอิมินเป็นสารทำ
ให้เสถียรที่ความเข้มข้น 1 ไมโครโมลาร์สามารถเหนี่ยวนำการแสดงออกของยีนได้อย่างมีนัยสำคัญ ($p \leq 0.05$) ใน
CYP1A1 และ CYP1A2 โดยมีค่าเท่ากับ 1.68 ± 0.35 และ 2.08 ± 0.56 เท่า ตามลำดับ สารผสมระหว่างนาโนพาร์
ทิเคิลของทองคำที่ใช้ซิเตรทเป็นสารทำให้เสถียรและสารเหนี่ยวนำการแสดงออกของยีน มีผลเหนี่ยวนำการ
แสดงออกของยีน CYP1A1, CYP1A2, CYP2C9 และ CYP3A4 ได้น้อยกว่าอย่างมีนัยสำคัญ ($p \leq 0.05$) เมื่อเทียบ
กับการใช้สารเหนี่ยวนำเพียงอย่างเดียว ในขณะที่สารผสมระหว่างนาโนพาร์ทิเคิลของทองคำที่ใช้โพลีเอททิลีน
อิมินเป็นสารทำให้เสถียรและสารเหนี่ยวนำการแสดงออกของยีน จะเหนี่ยวนำการแสดงออกของยีน CYP1A1,
CYP2C9 และ CYP3A4 ได้น้อยกว่าอย่างมีนัยสำคัญ ($p \leq 0.05$) เมื่อเทียบกับสารเหนี่ยวนำเพียงอย่างเดียว
นอกจากนั้นยังพบว่า สารผสมระหว่างนาโนพาร์ทิเคิลของทองคำที่ใช้โพลีเอททิลีนอิมินเป็นสารทำให้เสถียรที่
ความเข้มข้น 1 ไมโครโมลาร์และสารเหนี่ยวนำการแสดงออกของยีน สามารถเพิ่มการแสดงออกของยีน CYP1A2
ได้มากกว่าการใช้สารเหนี่ยวนำเพียงอย่างเดียวอย่างมีนัยสำคัญ ($p \leq 0.05$) ซึ่งผลของการเหนี่ยวนำการแสดงผล
ของยีนอาจขึ้นกับขนาดและประจุของนาโนพาร์ทิเคิลโดยชนิดที่ใช้โพลีเอททิลีนอิมินเป็นสารทำให้เสถียรมีขนาด
เล็กกว่านาโนพาร์ทิเคิลทองคำที่ใช้ซิเตรทเป็นสารทำให้เสถียรประมาณ 3 เท่า และมีประจุเป็นบวก ทำให้สามารถ
ผ่านเข้าเซลล์ได้ง่ายกว่าและมีผลเพิ่มการแสดงออกของยีนได้ดีกว่า อย่างไรก็ตามควรมีการศึกษาถึงกลไกในการ
เหนี่ยวนำการแสดงออกของยีนไซโตโครมพี 450 ของนาโนพาร์ทิเคิลทองคำเพิ่มเติมต่อไป

ภาควิชา..วิทยาการเภสัชกรรมและเภสัชอุตสาหกรรม... ลายมือชื่อนิสิต.....
สาขาวิชา...เทคโนโลยีเภสัชกรรม..... ลายมือชื่ออ.ที่ปรึกษาวิทยานิพนธ์หลัก.....
ปีการศึกษา...2553..... ลายมือชื่ออ.ที่ปรึกษาวิทยานิพนธ์ร่วม.....

507 68598 33: MAJOR PHARMACEUTICAL TECHNOLOGY

KEYWORDS: CYTOCHROME P450 / GOLD NANOPARTICLES / GENE EXPRESSION / INDUCTION

LADDEAR WANGCHAROENRUNG: EFFECT OF GOLD NANOPARTICLES ON CYTOCHROME P450 GENE EXPRESSION IN HEPG2 CELL LINE. THESIS ADVISOR: ASST. PROF. WARANGKANA WARISNOICHAROEN, Ph.D., THESIS CO-ADVISOR: PROF. APIWAT MUTIRANGURA, M.D., Ph.D., 95 pp.

Gold nanoparticles (AuNPs) have been recently used for many clinical applications including drug delivery, therapeutics and diagnostics. AuNPs were synthesized by using the chemical reduction method with different stabilizers, citrate and polyethyleneimine (PEI), the AuNPs were determined for their effect on human cytochrome P450 (CYP) mRNA induction, namely CYP1A1, CYP1A2, CYP2C9, CYP2E1 and CYP3A4, using real-time PCR technique. The average particle diameters of freshly prepared citrate- and PEI-stabilized AuNPs were 15.00 ± 2.77 and 5.02 ± 1.81 nm, respectively. The zeta potentials of citrate and PEI-stabilized AuNPs were -40.60 ± 1.22 and 8.10 ± 1.59 mV, in orderly. Citrate-stabilized AuNPs (AuCi) has shown to have no cytotoxicity on HepG2 cells at the maximum concentration of $90 \mu\text{M}$ whereas IC_{50} of PEI-stabilized AuNPs (AuPEI) was found to be $37.58 \pm 1.15 \mu\text{M}$. The significance in induction effect ($p \leq 0.05$) of AuCi at $10 \mu\text{M}$ observed on CYP1A2 and CYP2C9 was 2.32 ± 0.35 and 1.65 ± 0.39 folds, consecutively. AuPEI at a concentration of $1 \mu\text{M}$ significantly induced ($p \leq 0.05$) CYP1A1 and CYP1A2 up to 1.68 ± 0.35 and 2.08 ± 0.56 folds, respectively. The mixtures of AuNPs and CYP inducers, α -naphthoflavone for CYP1A and rifampicin for CYP2C9 and CYP3A4, decreased the effect of inducers significantly ($p \leq 0.05$) on CYP1A1, CYP1A2, CYP2C9 and CYP3A4 for AuCi, and on CYP1A1, CYP2C9 and CYP3A4 for AuPEI. Noticeably, the mixture of AuPEI at $1 \mu\text{M}$ and the inducer had a synergistic induction on CYP1A2 ($p \leq 0.05$). The potential of CYP induction of AuNPs seemed to depend upon the size and charge of AuNPs. AuPEI was about 3 times smaller in size than AuCi and contained positive charges which could support the cellular penetration. Nevertheless, the mechanism of CYP induction by AuNPs are suggested for further study.

Department:..Pharmaceutics and Industrial Pharmacy...	Student's Signature.....
Field of Study:....Pharmaceutical Technology.....	Advisor's Signature.....
Academic Year:....2010.....	Co-Advisor's Signature.....

ACKNOWLEDGEMENTS

I would like to express my honest pleasure to my thesis advisor, Assistant Professor Dr. Warangkana Warisnoicharoen for her precious advice, valuable guidance and cordially encouragement throughout my graduate study as well as her kindness, support and smile. I would like to express my grateful appreciation to my thesis co-advisor, Professor Dr. Apiwat Mutirangura (M.D.) for his useful suggestion, wisely guidance and kindness for the experiment work and presentation of the thesis. I would like to articulate my sincere appreciation to Dr. Amornpun Sereemaspu (M.D.) for his kind guidance and support on the experimental work. Also I would like to award my thankfulness and appreciation to Dr. Pithi Chanvorachote for his permission to use his cell laboratory room.

I would like to show admire to my thesis committee for their valuable comments and suggestions. I would like to give the special thanks to Dr. Narisorn Kongruttanachok for helping me throughout my experimental work. My thankfulness is also extended to Dr. Giulietta Spudich for his kind supportive and facilitation on the designing of primers. I would like to thank the Faculty of Graduate Studies, Chulalongkorn University for partial support of the scholarship which enabled me to undertake this study.

Thanks are expressed to my colleagues and friends in the Faculty of Pharmaceutical Sciences and the Faculty of Medicine, Chulalongkorn University for their encouragement and understanding. I am really thankful to my beloved family for educational opportunity, supporting, inspiration, love, care and understanding. Finally, I would like to extend my thankfulness and gratitude to whom whose names are not mentioned here for helping me in everything.

CONTENTS

	Page
ABSTRACT (THAI)	iv
ABSTRACT (ENGLISH)	v
ACKNOWLEDGEMENTS	vi
CONTENTS	vii
LIST OF TABLES	xi
LIST OF FIGURES	xii
LIST OF ABBREVIATIONS	xvi
CHAPTER	
I INTRODUCTION	1
1. Background and significance of the study.....	1
2. Objectives of the study.....	5
II LITERATURE REVIEW	6
1. Nanotechnology.....	6
2. Gold nanoparticles.....	6
2.1 Pharmaceutical application of gold nanoparticles.....	8
2.2 Cellular uptake of gold nanoparticles.....	9
2.3 Cytotoxicity of gold nanoparticles.....	10
3. Metabolic pathway.....	11
4. Cytochrome P450.....	12
4.1 The main human CYP isozymes.....	13

CHAPTER	Page
4.1.1 CYP1A1.....	13
4.1.2 CYP1A2.....	14
4.1.3 CYP2C9.....	14
4.1.4 CYP2E1.....	14
4.1.5 CYP3A4.....	15
4.2 Induction of drug metabolism.....	18
4.2.1 CYP1A induction.....	19
4.2.2 CYP2C induction.....	20
4.2.3 CYP3A induction.....	21
4.2.4 CYP2E1 induction.....	22
III MATERIALS AND METHODS.....	23
1. Materials.....	23
1.1 Equipment.....	23
1.2 Chemicals.....	24
2. Methods.....	27
2.1 Preparation of gold nanoparticles.....	27
2.2 Characterization of gold nanoparticles.....	29
2.2.1 UV – visible spectroscopy.....	29
2.2.2 Zeta potential measurement	30
2.2.3 Size and size distribution	31
2.3 Cell line and cell culture.....	31

CHAPTER	Page
2.4 Cytotoxicity test of gold nanoparticles.....	32
2.5 Detection of CYP gene in HepG2 cell line.....	33
2.5.1 RNA extraction.....	33
2.5.2 Synthesis of cDNA.....	34
2.5.3 Gene expression assay.....	34
2.5.3.1 Primer selection.....	34
2.5.3.2 Polymerase chain reaction (PCR).....	36
2.5.3.3 Gel electrophoresis.....	37
2.5.3.3.1 Gel preparation.....	37
2.5.3.3.2 Electrophoresis.....	37
2.6 Investigation of AuNPs influence on CYP mRNA expression.....	38
2.6.1 Treatment of cultures.....	38
2.6.2 RNA extraction.....	38
2.6.3 Gene expression assay.....	39
2.6.3.1 Amplification with real-time performance....	39
2.6.3.2 Data analysis with $2^{-\Delta\Delta Ct}$ method.....	39
2.7 Statistical analysis.....	40
IV RESULTS AND DISCUSSION.....	41
1. Characterization of gold nanoparticles.....	41
1.1 Appearances.....	41

CHAPTER	Page
1.2 UV-visible spectroscopy.....	44
1.3 Zeta potential measurement.....	48
1.4 Size and size distribution.....	49
2. Cytotoxicity test.....	55
3. Verification of CYP gene in HepG2 cell line.....	57
4. Investigation of gold nanoparticles influence on CYP mRNA expression.....	59
4.1 CYP1A1.....	59
4.2 CYP1A2.....	61
4.3 CYP2C9.....	63
4.4 CYP2E1.....	63
4.5 CYP3A4.....	66
V CONCLUSION.....	75
REFERENCES.....	77
APPENDICES.....	90
APPENDIX A.....	91
APPENDIX B.....	92
APPENDIX C.....	93
BIOGRAPHY.....	95

LIST OF TABLES

Table		Page
1	Cytochrome P450 enzymes and their substrates, inhibitors and inducers.....	16
2	Primer sequences for CYP1A1, CYP1A2, CYP2C9, CYP2E1, CYP3A4 and GAPDH.....	36
3	Gel electrophoresis of PCR products of CYP genes with different annealing temperatures.....	58
4	UV absorption of citrate and PEI-stabilized AuNPs after preparation and 1 month storage.....	88
5	Viability of HepG2 cells after incubated with AuCi for 48 h.....	89
6	Viability of HepG2 cells after incubated with AuPEI for 48 h.....	89
7	Fold induction of CYP genes in HepG2 cells after incubation with inducer or AuNPs.....	90
8	Fold induction of CYP genes in HepG2 cells after incubation with a mixture of inducer and AuNPs.....	91

LIST OF FIGURES

Figure	Page
1	Differences in colors of gold nanospheres in different sizes and gold nanorods in different aspect ratios due to the nature of plasmon bands.....7
2	Cells incubated with gold nanorod, embedded in resin for TEM analysis.....9
3	TEM image of Panc-I cells treated with gold nanoparticles.....10
4	Structure showing the heme moiety in cytochrome P450.....13
5	Mechanism of CYP1A1 and CYP1A2 gene transcription activation.....19
6	Mechanism of CYP2C9 gene transcription activation.....20
7	Mechanism of CYP3A4 gene transcription activation.....21
8	Synthesis of citrate stabilized gold nanoparticles with 3 different conditions as indicated in bracelets.....28
9	Synthesis of polyethyleneimine stabilized gold nanoparticles with 3 different conditions as indicated in bracelets.....28
10	The appearances of citrate-stabilized AuNPs after synthesis (A) and 1 month storage (B), PEI-stabilized AuNPs after synthesis (C) and after one month storage (D), prepared using conditions 1, 2 and 3.....43
11	UV absorption spectra of citrate-stabilized AuNPs prepared with condition 1 after preparation and 1 month storage.....45
12	UV absorption spectra of citrate-stabilized AuNPs prepared with condition 2 after preparation and 1 month storage.....45

Figure	Page
13 UV absorption spectra of citrate-stabilized AuNPs prepared with condition 3 after preparation and 1 month storage.....	46
14 UV absorption spectra of PEI-stabilized AuNPs prepared with condition 1 after preparation and 1 month storage.....	46
15 UV absorption spectra of PEI-stabilized AuNPs prepared with condition 2 after preparation and 1 month storage.....	47
16 UV absorption spectra of PEI-stabilized AuNPs prepared with condition 3 after preparation and 1 month storage.....	47
17 TEM images of citrate-stabilized AuNPs after preparation (A, B) and 1 month storage (C, D).....	51
18 TEM images of PEI-stabilized AuNPs after preparation (A, B) and 1 month storage (C, D).....	52
19 Size distributions of citrate-stabilized AuNPs after preparation (A) 1 month storage (C, D).....	53
20 Size distributions of PEI-stabilized AuNPs after preparation (A) 1 month storage (C, D).....	54
21 Cytotoxicity test of AuCi on HepG2 cells.....	56
22 Cytotoxicity test of AuPEI on HepG2 cells.....	56
23 Fold induction of α NF (inducer), AuCi (1 and 10 μ M), AuPEI (0.1 and 1 μ M), and DMSO on CYP1A1 gene in HepG2 cells.....	60

Figure	Page
24 Fold induction of α NF (inducer), AuCi 1 μ M + α NF, AuCi 10 μ M + α NF, AuPEI 0.1 μ M + α NF, and AuPEI 1 μ M + α NF on CYP1A1 gene in HepG2 cells.....	60
25 Fold induction of α NF (inducer), AuCi (1 and 10 μ M), AuPEI (0.1 and 1 μ M), and DMSO on CYP1A2 gene in HepG2 cells.....	62
26 Fold induction of α NF (inducer), AuCi 1 μ M + α NF, AuCi 10 μ M + α NF, AuPEI 0.1 μ M + α NF, and AuPEI 1 μ M + α NF on CYP1A2 gene in HepG2 cells.....	62
27 Fold induction of Rif (inducer), AuCi (1 and 10 μ M), AuPEI (0.1 and 1 μ M), and DMSO on CYP2C9 gene in HepG2 cells.....	64
28 Fold induction of Rif (inducer), AuCi 1 μ M + Rif, AuCi 10 μ M + Rif, AuPEI 0.1 μ M + Rif, and AuPEI 1 μ M + Rif on CYP2C9 gene in HepG2 cells.....	64
29 Fold induction of EtOH (inducer), AuCi (1 and 10 μ M), AuPEI (0.1 and 1 μ M), and DMSO on CYP2E1 gene in HepG2 cells.....	65
30 Fold induction of EtOH (inducer), AuCi 1 μ M + EtOH, AuCi 10 μ M + EtOH, AuPEI 0.1 μ M + EtOH, and AuPEI 1 μ M + EtOH on CYP2E1 gene in HepG2 cells.....	65
31 Fold induction of Rif (inducer), AuCi (1 and 10 μ M), AuPEI (0.1 and 1 μ M), and DMSO on CYP3A4 gene in HepG2 cells.....	67

Figure	Page
32 Fold induction of Rif (inducer), AuCi 1 μ M + Rif, AuCi 10 μ M + Rif, AuPEI 0.1 μ M + Rif, and AuPEI 1 μ M + Rif on CYP3A4 gene in HepG2 cells.....	67
33 Fold induction of AuCi 1 μ M and AuCi 10 μ M on CYP1A1, CYP1A2, CYP2C9, CYP2E1 and CYP3A4 gene in HepG2 cells.....	71
34 Fold induction of AuPEI 0.1 μ M and AuPEI 1 μ M on CYP1A1, CYP1A2, CYP2C9, CYP2E1 and CYP3A4 gene in HepG2 cells.....	71
35 Fold induction of AuCi 1 μ M and AuPEI 1 μ M on CYP1A1, CYP1A2, CYP2C9, CYP2E1 and CYP3A4 gene in HepG2 cells.....	72

LIST OF ABBREVIATIONS

°C	degree Celsius
α NF	alpha-naphthoflavone
Δ	delta (difference)
ϵ	dielectric constant
Ω	ohm
λ_{\max}	maximum absorbance wavelength
μ g	microgram
μ M	micromolar
μ L	microlitter
η	viscosity
ζ	zeta potential
AHR	aryl hydrocarbon receptor
AIP	actin cortical patch component
ARNT	aryl hydrocarbon receptor nuclear translocator
ATCC	American Type Culture Collection
AuCi	citrate-stabilized gold nanoparticle
AuNPs	gold nanoparticles
AuPEI	polyethyleneimine-stabilized gold nanoparticles
bFGF	basic fibroblast growth factor

CAR	constitutive androstane receptor
CCRP	constitutive androstane receptor retention protein
cDNA	complementary deoxyribonucleic acid
CLL	chronic lymphocytic leukemia
cm ²	square centimeter
Cont.	continue
C _t	cycle threshold
CYP	cytochrome P450
<i>d</i>	diameter of the sphere
DEPC	diethylpyrocarbonate
DMSO	dimethylsulfoxide
DNA	deoxyribonucleic acid
dNTP	nucleotides
<i>et al.</i>	<i>et alii</i> (and others)
<i>etc.</i>	<i>et cetera</i> (and other similar things)
EtOH	ethanol
GAPDH	glyceraldehyde 3-phosphate dehydrogenase
h	hour
HSP90	heat-shock protein
IC ₅₀	median (50%) inhibitory concentration
M	molar
mg	milligram

min	minute
mL	milliliter
mM	millimolar
mV	millivolt
mRNA	messenger ribonucleic acid
MW	molecular weight
NADPH	nicotinamide adenine dinucleotide phosphate
nm	nanometer
nM	nanomolar
Pa	Pascal
PAH	polycyclic aromatic hydrocarbon
PBREM	phenobarbitone-responsive enhancer module
PCR	polymerase chain reaction
PBS	phosphate buffered saline
PEI	polyethyleneimine
PP-2A	protein phosphatase 2A
ppm	part per million
PXR	pregnane X receptor
Rif	rifampicin
ROX	6-carboxyl-X-rhodamine
RNA	ribonucleic acid
RNase	ribonuclease

rpm	revolutions per minute
RT	reverse transcriptase
RXR	retinoic acid X receptor
sec	second
SD	standard deviation
SPR	surface plasmon resonance
TBE	tris-boric ethylenediaminetetraacetic acid
TEM	transmission electron microscopy
U	unit
U_E	electrophoretic mobility
UV	ultraviolet
v	volume
VEGF	vascular endothelial growth factor
XRE	xenobiotic response elements

CHAPTER I

INTRODUCTION

1. Background and significance of the study

Gold nanoparticles (AuNPs) are gold particles in nanoscale size ranging from 1 to 100 nm. The gold colloids are used in the treatment of rheumatoid arthritis for decades (Aaseth, Haugen and Forre, 1998). In these days, the advanced availability of technology support studies in more details of the nanoparticles. Specific physical and chemical properties of gold particles are the color changing when the size is altered, light absorbance at 520 nm, ability to conduct electricity and catalytic activity. The AuNPs are normally coated with suspending agents such as citrate and polyethyleneimine in order to enhance the stability (Bhattacharya and Mukherjee, 2008).

Due to their small sizes, the nanoparticles are believed to be capable of penetrating into cells easily through the small capillary pores within the human vasculature (Mukherjee *et al.*, 2005). They have brought in various biomedical applications, including detection and identification (Alivisatos, 2004; You *et al.*, 2007), diagnosis (El-Sayed, Huang, and El-Sayed, 2005; Zharov *et al.*, 2005), therapeutics (El-Sayed, Huang and El-Sayed, 2006; Mukherjee *et al.*, 2007; Patra *et al.*, 2008) and imaging (Sokolov *et al.*, 2003).

Effects of AuNPs and other nanoparticles on the cellular function and cytotoxicity recently have been concerned and evaluated prior to clinical use. Goodman *et al.* (2004) measured viability of COS-1 cells treated with different cationic and anionic AuNPs. The results showed IC_{50} of $1 \pm 0.5 \mu M$ in quaternary

ammonium functionalized AuNPs and more than 7.37 μM in carboxylic acid-substituted AuNPs. In 2005, Shukla *et al.* incubated 100 μM of AuNPs capped by lysine and poly-L-lysine with macrophage cells for 72 hours and found that cell viability was decreased to 85%. It seemed that, cytotoxicity of AuNPs varied with suspending agents (Murphy *et al.*, 2008).

Apart from toxicity studies, biological studies of the AuNPs including effects on cellular protein function or protein synthesis were reported. There are two main steps involved in a cellular protein synthesis. Firstly, a gene provides the instructions for synthesizing a messenger RNA (mRNA) molecule or gene transcription. Next step, a specific polypeptide is synthesized from mRNA using ribosomes. Therefore, mRNA expression results in protein availability in the cells (Lewin, 2008). AuNPs were able to down-regulate the activity of heparin-binding glycoproteins, vascular endothelial growth factor and heparin-binding growth factor (Mukherjee *et al.*, 2005). These proteins are found in cancer cells and responsible for cancer proliferation. Similarly, AuNPs were found to inhibit cell proliferation in G1 phase of the cell cycle in eukaryotes (Bhattacharya *et al.*, 2007).

Some studies showed more evidences of nanosystems affecting the transcriptional level of protein synthesis or gene expression. Zhang *et al.* (2006) examined silica-coated CdSe/ZnS quantum dots terminated with both thiol and PEG functional groups on gene expression. For human skin fibroblasts (HSF-42) treated with 8 and 80 nM quantum dots, 50 genes exhibited statistically significant changes in expression level of greater than 2-fold. In 2007, Papis *et al.* exposed BALB3T3 fibroblasts with cobalt nanoparticles and evaluated the gene expression. They found that approximately 24% of genes investigated were differentially expressed.

Altogether, these evidences support the existence of nanoparticle influence on gene expression.

Cellular effects of AuNPs on the expression of genes have also been studied. There was an experiment of Khan *et al.* (2007) which showed that the citrate-capped gold nanospheres were able to internalize into the cells. However, the significant change in gene-expression patterns was not observed. Hauck, Ghazani and Chan (2008) examined gene-expression profiles with gold nanorod uptake in mammalian cells. The results showed that some genes had differential expression after nanorod exposure. These genes were mainly involved in apoptosis, cell cycle regulation, cellular metabolism and electron transport system. Nevertheless, none of metabolizing enzymes especially cytochrome P450 have been investigated for gene expression with a challenge of gold nanoparticles.

Cytochrome P450 (CYP) is the protein family involved in the metabolism of drug and xenobiotics. It is also related to the drug interactions and toxicities. There are three main families of the enzyme classified; CYP 1, 2 and 3. Followings are details of some important CYPs in humans.

CYP1A1 oxidizes planar aromatic which are multiples of benzene or so-called polycyclic aromatic hydrocarbons (PAHs). High levels of this CYP were found in smokers and breast cancer patients. CYP1A2 originates from a gene on chromosome 15 in humans. CYP1A2 is capable to oxidize planar aromatic molecules that contain aromatic amines such as series of oestrogen hormones, caffeine and theophylline. It can be blocked by methylxanthine derivative, furafylline (Coleman, 2005).

For CYP2C9, its structure makes up a large active site and more than one active sites are found, resulting in a large number of its substrates. Cimetidine

fluconazole, isoniazid or omeprazole, for instances, are its inhibitors where it can be induced by rifampicin and phenobarbital (Goshman, Fish and Roller, 1999).

CYP2E1 is the only member of the CYP2E subfamily in humans and found approximately 7% in liver. Besides, it is also expressed in extrahepatic tissues including lungs and brain. Ethanol is the potent inducer for this CYP enzyme (Coleman, 2005).

CYP3A4 is responsible for metabolism of over 120 drugs (Coleman, 2005). Its major function is to metabolize steroids. Nevertheless, because of its huge and flexible active site, varieties of different molecules can undergo at least some metabolism by this enzyme. Erythromycin is a common substrate of CYP3A4 metabolism while anticonvulsants, St John's Wort, phenytoin and rifampicin are its inducible molecules.

Since AuNPs are promising candidate for medical applications, the toxicity evaluation of the nanoparticles prior to clinical use would be of great interest. The first mechanism against xenobiotics is the metabolism by cytochrome P450. Thus, investigating the effects of AuNPs on CYPs is beneficial for the use of AuNPs. Furthermore, the variety of applications might bring co-administration of AuNPs with other drugs. Therefore, in the present study, gold nanoparticles decorated with citrate and polyethyleneimine were synthesized, characterized and determined for the cytotoxicity and the biological effect on mRNA expression of CYPs (CYP1A1, CYP1A2, CYP2C9, CYP2E1 and CYP3A4) on human hepatoma cell line, HepG2.

2. Objectives of the study

- 2.1 To prepare and characterize gold nanoparticles
- 2.2 To investigate the non-toxic concentration range of gold nanoparticles on HepG2 cell line
- 2.3 To investigate the effect of gold nanoparticles on the expression of human cytochrome P450 genes

CHAPTER II

LITERATURE REVIEW

1. Nanotechnology

Over the recent decades, nanotechnology has drawn much interest in many fields as the results of developed technology and the abilities of utilities. Working on an atomic or molecular scale creates nanomaterials such as nanotubes, nanowires, nanocrystals, nanoparticles and quantum dots which consist of novel properties. The nanotechnology has opened up the world beyond microscale which is relevant to treatment, diagnosis and development of new drugs including tailoring of materials in an atomic scale as a nanoparticle.

2. Gold nanoparticles

Gold nanoparticles (AuNPs) exhibit significantly distinct physical, chemical and biological properties from their bulk counterparts. The optical properties of metal nanoparticles are conquered by collective oscillations of electrons (plasma oscillations) that are in resonance with the incident electromagnetic radiation. The oscillations of AuNPs are governed by their bulk dielectric constant which gives the visible region of the electromagnetic spectrum (El-Sayed, 2001). Changes in surrounding of AuNPs such as aggregation and medium refractive index result in colorimetric changes of the dispersions as seen in Figure 1 (Burda *et al.*, 2005; Murphy *et al.*, 2008).

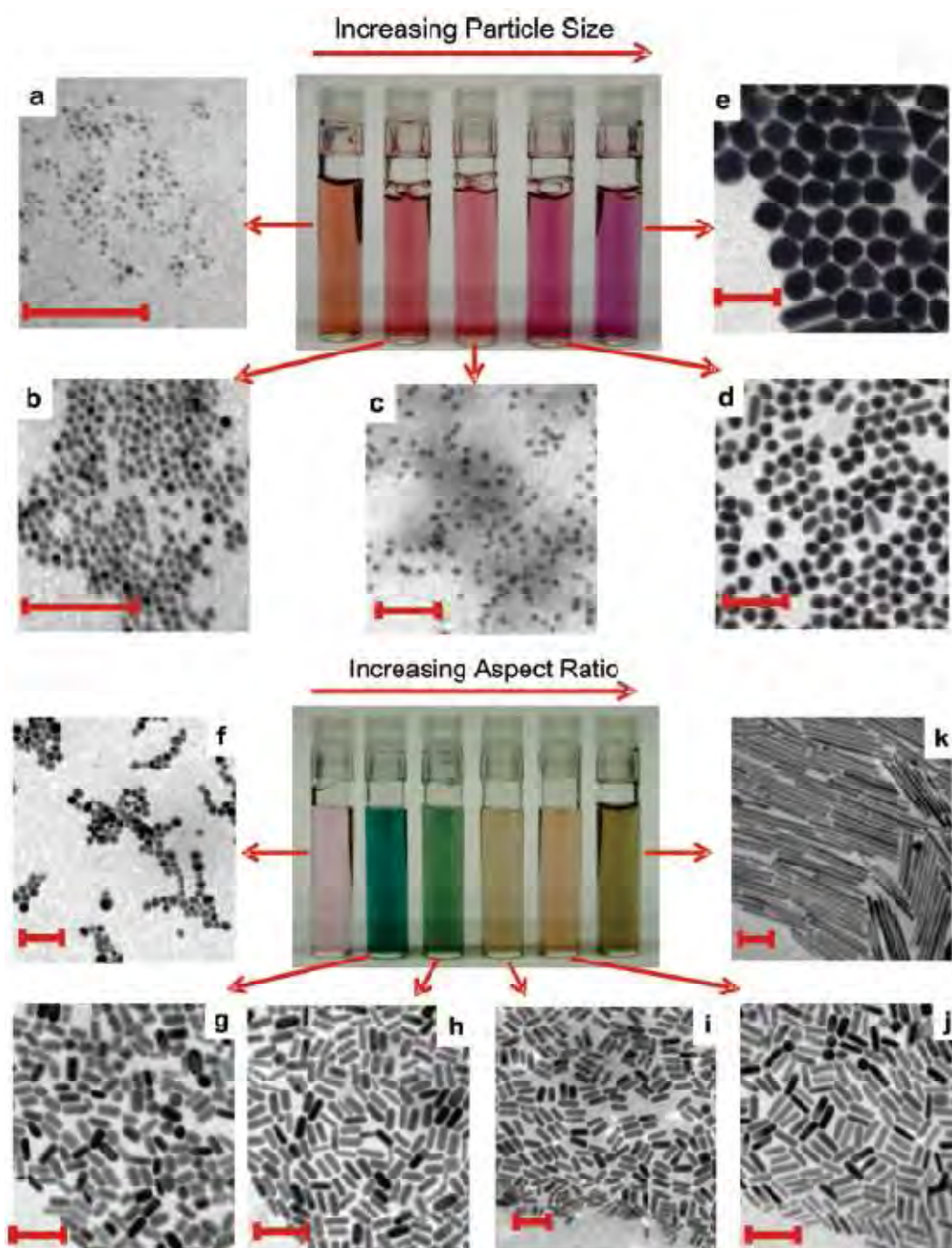


Figure 1 Differences in colors of gold nanospheres in different sizes (upper panels, a-e) and gold nanorods in different aspect ratios (lower panels, f-k) due to the nature of plasmon bands (all scale bars = 100 nm) (Murphy *et al.*, 2008)

2.1 Pharmaceutical application of gold nanoparticles

The unique physical and chemical properties of AuNPs brought to various pharmaceutical applications, therapeutics, drug delivery, imaging, detection and identification. There were many reports supporting the uses of AuNPs themselves in therapeutic applications. One report showed that AuNPs selectively inhibited vascular endothelial growth factor (VEGF)-165 and basic fibroblast growth factor (bFGF) that led to a decrease in proliferative activity in angiogenesis (Mukherjee *et al.*, 2005). AuNPs have an ability to inhibit the proliferation multiple myeloma cell lines and were able to induce apoptosis in chronic lymphocytic leukemia (CLL) B cells (Bhattacharya *et al.*, 2007; Mukherjee *et al.*, 2007).

AuNPs are able to use as non-toxic carriers for drug and gene delivery applications. Not only because of the gold core is inert and non-toxic, the surface of AuNPs are also can be tailored by functional ligand presenting ability to objective a specific target (Ghosh *et al.*, 2008). An example of drug carrier is the use of AuNPs conjugated with paclitaxel targeting on cancer cells by using an advantage of the small sizes of particles that could avoid the reticuloendothelial system (Gibson, Khanal and Zubarev, 2007). A delivery of DNA into cells was carried out using oligonucleotide-modified nanoparticles which were stable against enzymatic digestion (Rosi *et al.*, 2006). The use of AuNPs in imaging application was done by attaching the particles with probe molecules to give specific contrast agents for imaging (Sokolov *et al.*, 2003). AuNPs were used to detect the presence of specific mRNA from a total RNA extract of yeast cells by linking AuNPs with DNA (Baptista *et al.*, 2007).

2.2 Cellular uptake of gold nanoparticles

There are many evidences showing cellular uptake of AuNPs while the cells are alive. Due to their small sizes, Mukherjee *et al.* (2005) proposed that the nanoparticles are capable to penetrate into cells easily through the small capillary pores within the human vasculature.

In 2008, Hauck, Ghazani and Chan showed gold nanorods presented in HeLa cell after incubation with nanorods for 6 h (Figure 2) and suggested that reaction of cellular uptake may cause by charge of particles. From the results, positive charged particles exhibit the higher uptake into HeLa cells due to electrostatic interaction.

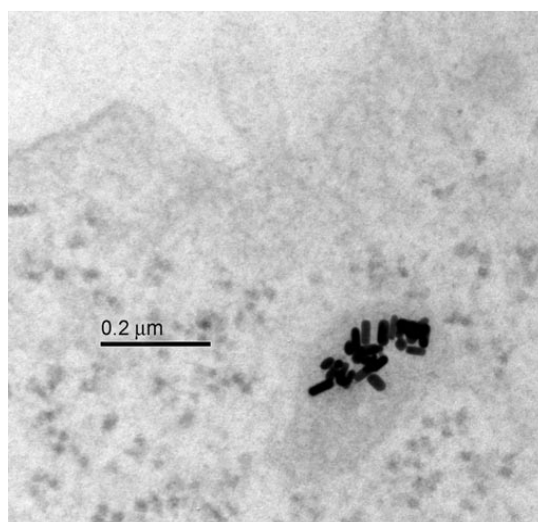


Figure 2 Cells incubated with gold nanorod, embedded in resin for TEM analysis (Hauck, Ghazani and Chan, 2008)

Another study suggested that gold nanoparticles were taken into human pancreatic carcinoma cell line (Panc-I) *in vitro* by endocytosis with an evidence of cytoplasmic vesicles containing gold nanoparticles as shown in Figure 3 (Gannon *et al.*, 2008).

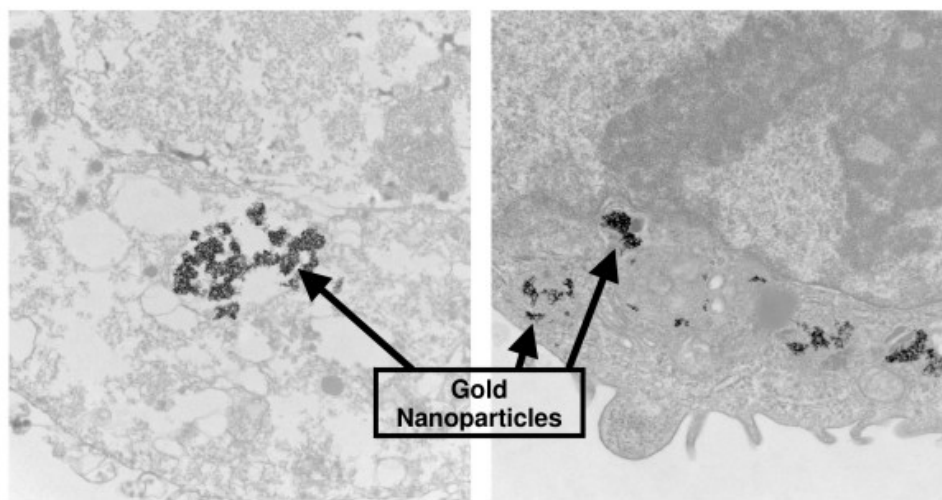


Figure 3 TEM image of Panc-I cells treated with gold nanoparticles (Gannon *et al.*, 2008)

When gold nanoparticles are capable to be inside the cells, there will be a chance of gold nanoparticles to interact with proteins in cells and might cause cell death. Thus, cytotoxicity of AuNPs is also an important issue to be studied.

2.3 Cytotoxicity of gold nanoparticles

Since there are many applications of gold nanoparticles, cellular toxicity of gold nanoparticles were concerned and examined. Goodman *et al.* (2004) measured viability of COS-1 cells treated with different cationic and anionic AuNPs. The results showed IC_{50} of $1 \pm 0.5 \mu\text{M}$ in quaternary ammonium functionalized AuNPs (cationic AuNPs) and more than $7.37 \mu\text{M}$ in carboxylic acid-substituted AuNPs (anionic AuNPs). In 2005, Shukla *et al.* incubated $100 \mu\text{M}$ of AuNPs capped by lysine and poly-L-lysine with macrophage cells for 72 h and found that cell viability

was decreased to 85%. Hence, the cytotoxicity of AuNPs might be varied with stabilizer (Murphy *et al.*, 2008).

3. Metabolic pathway

Many drugs or toxins that invade living systems should be transformed through phases I, II and III of the metabolic pathway. Each phase responses for different action as described below (Chiu, 1993).

Phase I: functionalization

The functionalization is done by an introduction of a polar group into the drug molecule by many reactions which are oxidation, reduction, hydrolysis, hydration, dethioacetylation, and isomerization. Enzyme responsible for this phase is cytochrome P450.

Phase II: conjugation

The conjugation is done by an attachment of a small, polar and ionizable endogenous compound into the drug molecule by glucoronidation/glucosidation, sulfation, amino acid conjugation, glutathione conjugation, condensation, fatty acid conjugation, acetylation, and methylation.

Phase III: efflux transportation

The last phase of metabolization is to transport the metabolite out of the cells in urine or bile by the efflux pump systems.

4. Cytochrome P450

Cytochrome P450 (CYP) is a group of heme-thiolate enzymes responsible for the functionalization of a substrate in phase I of metabolic pathway. The CYP superfamily consists of over 5500 sequences from which only 57 was found in human (Nelson *et al.*, 2004). They are synthesized mainly in the endoplasmic reticulum of the liver and the lesser of them devote to small intestine, kidney, adrenals lung, heart, brain and other tissues (Guengerich, 2004). Currently, CYPs are classified by according to their amino acid sequence homology. The same family of CYPs should contain at least 40% of their amino acid structure in common which are classified by number as CYP1, CYP2 and CYP3. If the structures have 55% sequence homology, they are in the same subfamily, classified by alphabet, CYP1A, CYP2A, CYP2B etc. Finally, a number was given to individual isoforms which originate from a single gene such as CYP1A2, CYP1A2.

The CYP contains hydrophobic pocket containing hundreds of amino acid residues which attract a substrate by forces including van der Waals', pi-pi and hydrogen bonding. Below the hydrophobic pocket is the heme moiety which is the key structure of the CYP. The moiety contains ferriprotoporphyrin-9 binding to five other molecules in horizontal plane (Figure 4). The iron is crucial to the catalytic function of CYP enzymes in order to oxidize their substrates which require electrons from nicotinamide adenine dinucleotide phosphate (NADPH) as showed in the following equation (Bibi, 2008)



where, RH = oxidisable drug substrate

ROH = hydroxylated metabolite

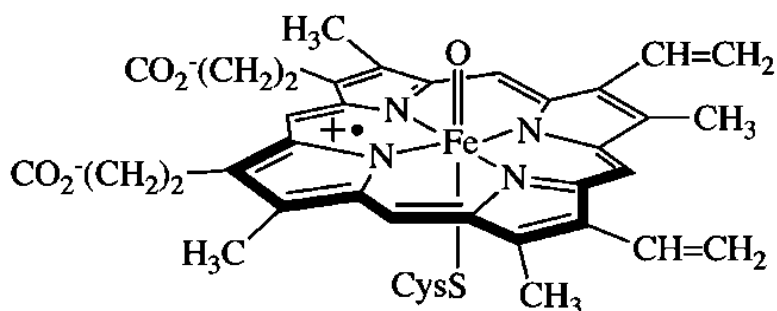


Figure 4 Structure showing the heme moiety in cytochrome P450 (Shaik *et al.*, 2010)

4.1 The main human CYP isozymes

4.1.1 CYP1A1

CYP1A1 has been studied extensively because of their roles in activation of carcinogens. Cigarette smokers exhibit high levels of this CYP in their lungs (Dorrenhaus, Muller and Roos, 2007). The CYP is mainly involved in polycyclic aromatic hydrocarbon (PAH) metabolism such as benzo[a]pyrene, 3-methylcholanthrene, and naphthalene (Roberts-Thomson *et al.*, 1993). Induction of CYP1A1 is under the regulation of *Ah* locus which is induced through aryl hydrocarbon receptor (AHR)/AHR nuclear translocator (ARNT) heteromeric complexes. Drugs including meprazole, nimodipine, leflunomide, mexiletine, atorvastatin, and flutamide are CYP1A1 inducers.

4.1.2 CYP1A2

CYP1A2 originates from a gene on chromosome 15 in humans. It is capable of oxidizing planar aromatic molecules that contain aromatic amines such as series of oestrogen hormones, caffeine and theophylline. Similar to CYP1A1, PAHs are also inducers of CYP1A2. It can be blocked by methylxanthine derivative (Coleman, 2005). There is an evidence showing that elevated levels of CYP1A2 can be a predisposing factor to colorectal cancer (Kiss *et al.*, 2007).

4.1.3 CYP2C9

The structure of CYP2C9 makes up a large active site and more than one active site are found, resulting in a large number of its substrates. CYP2C9 metabolizes about 16% of clinically important drugs including narrow therapeutic drugs such as (S)-warfarin, phenytoin and tolbutamide (Schwarz, 2003). Cimetidine, fluconazole, isoniazid or omeprazole, for instances, are its inhibitors where it can be induced by rifampicin and phenobarbital (Goshman, Fish and Roller, 1999).

4.1.4 CYP2E1

CYP2E1 is the only member of the CYP2E subfamily in humans and found approximately 7% in liver. Besides, it is also expressed in extrahepatic tissues including lung, kidney, brain, nasal mucosa, bone marrow and peripheral blood lymphocytes. Expression of the CYP is altered in response to a variety of xenobiotics as well as physiological conditions including starvation, obesity, diabetes, and carcinoma (Coleman, 2005). Substrates of this enzyme are small heterocyclic agents

and ketones such as acetaminophen, ethanol, chlorzoxazone and halothane (Goshman, Fish and Roller, 1999). In addition, ethanol and acetone are the potent inducers for this CYP (Coleman, 2005).

4.1.5 CYP3A4

CYP3A4 is the most abundant of the CYP enzymes in the liver which is major important in human biology and clinical therapeutics and it is responsible for metabolism of over 150 drugs. Its major function is to metabolize steroids. Nevertheless, because of its huge and flexible active site, varieties of different molecules can undergo at least some metabolism by this enzyme. Drugs metabolized through the enzyme including most calcium channel blockers, erythromycin, benzodiazepines, cyclosporine and tacrolimus. Potent inhibitors of CYP3A4 are macrolides and imidazole antibiotics while anticonvulsants, St John's Wort, phenytoin and rifampicin are its inducible molecules (Coleman, 2005; Goshman, Fish and Roller, 1999).

Overall of cytochrome P450 enzymes along with their substrates, inhibitors and inducers are summarized in Table 1.

Table 1 Cytochrome P450 enzymes and their substrates, inhibitors and inducers (Goshman, Fish and Roller, 1999)

Isozyme	Substrates	Inhibitors	Inducers
CYP1A1	PAHs Heterocyclic amines Estradiol	α -Naphthoflavone Isoniazid Pinostilbene Pterostilbene Desoxyrhapontigenin	PAHs Tetrachlorodibenzo-dioxin α -Naphthoflavone β -Naphthoflavone Atorvastatin Flutamide Leflunomide Mexiletine Nimodipine Omeprazole Smoking
CYP1A2	Caffeine Clozapine Cyclobenzaprine Fluvoxamine Imipramine Mexiletine Propranolol Theophylline	α -Naphthoflavone Cimetidine Ciprofloxacin Clarithromycin Enoxacin Erythromycin Fluvoxamine Ofloxacin Ticlopidine	PAHs Tetrachlorodibenzo-dioxin α -Naphthoflavone β -Naphthoflavone Omeprazole Smoking

Table 1 (Cont.)

Isozyme	Substrates	Inhibitors	Inducers
CYP2C9	Diclofenac Flurbiprofen Ibuprofen Losartan Mefenamic acid Naproxen Phenytoin Piroxicam Sulfamethoxazole Tolbutamide Warfarin	Amiodarone Fluconazole Fluoxetine Isoniazid Paroxetine Sulfafenazole Ticlopidine	Phenobarbital Rifampin
CYP2E1	Acetaminophen Chlorzoxazone Dapsone Ethanol Enflurane Isoflurane Paracetamol Salicylic acid	Disulfiram	Ethanol Isoniazid

Table 1 (Cont.)

Isozyme	Substrates	Inhibitors	Inducers
CYP3A	Alprazolam Astemizole Buspirone Carbamazepine Cisapride Cyclosporine Diazepam Erythromycin Protease inhibitors Lovastatin Midazolam Nifedipine Omeprazole Simvastatin Tamoxifen Testosterone Verapamil	Amiodarone Cimetidine Clarithromycin Erythromycin Grapefruit juice Itraconazole Ketoconazole	Carbamazepine Glucocorticoids Phenytoin Rifampin Ritonavir

4.2 Induction of drug metabolism

Drugs or ligands which are capable of binding with nuclear receptors can bring to CYP induction. The main receptors are aryl hydrocarbon receptor (CYP1A), pregnane X receptor (CYP3A), and constitutive androstane receptor (CYP2C). Nevertheless, CYP2E1 induction are not related to receptor but otherwise, related to post-transcriptional level (Tsutsumi, Lasker, and Takahashi, 1993; Hukkanen, 2000; Coleman, 2005).

4.2.1 CYP1A induction

The activation of CYP1A1 and CYP1A2 mRNA expression is a process via aryl hydrocarbon receptor (AHR) which can be found in the cytoplasm of most cells. The receptor maintained in a complex containing heat-shock protein (HSP90) and actin cortical patch component (AIP). When it binds to an AHR ligand, it migrates to the nucleus and leaves chaperon proteins behind in the cytoplasm. In nucleus, the complex binds to AHR nuclear translocator (ARNT) and then binds to the xenobiotic response elements (XRE) of CYP genes activating transcription (Figure 5) (Kawajiri and Fujii-Kuriyama, 2007). It is thought that PAHs and heterocyclic amines induce CYP1A1 and 1A2 in this way as well as the anti-ulcer agent, omeprazole (Coleman, 2005).

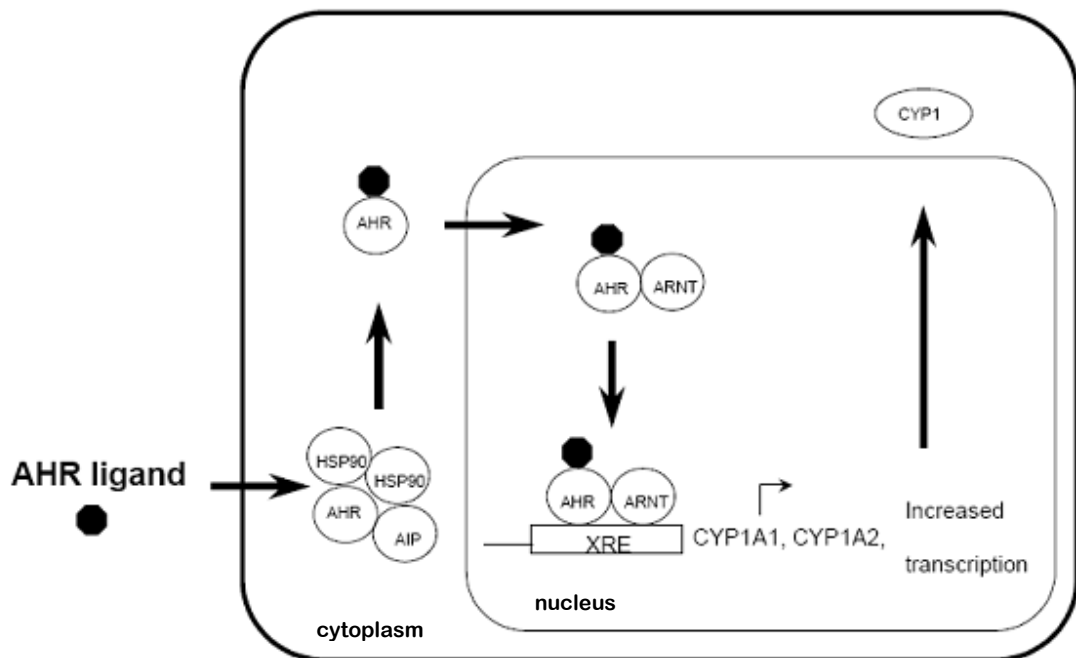


Figure 5 Mechanism of CYP1A1 and CYP1A2 gene transcription activation (Hukkanen, 2000)

4.2.2 CYP2C induction

CYP2C is controlled by constitutive androstane receptor (CAR) which is predominantly expressed in the liver. Normally, CAR is in complex with Hsp90 and the cochaperone cytoplasmic CAR retention protein (CCRP). Once a ligand binds to CAR and subsequently recruits protein phosphatase 2A (PP-2A) to the complex and move into the nucleus. The complex binds to retinoic acid X-receptor (RXR) before binding to phenobarbitone-responsive enhancer module (PBREM), and then activates gene transcription (Figure 6) (Swales and Negishi, 2004).

The CAR ligands include phenobarbitone, phenytoin and rifampicin. On the other hand, CAR is deactivated through the release of the SRC-1 from the ligand-binding domain by deactivators such as cytokines and some steroids (Coleman, 2005).

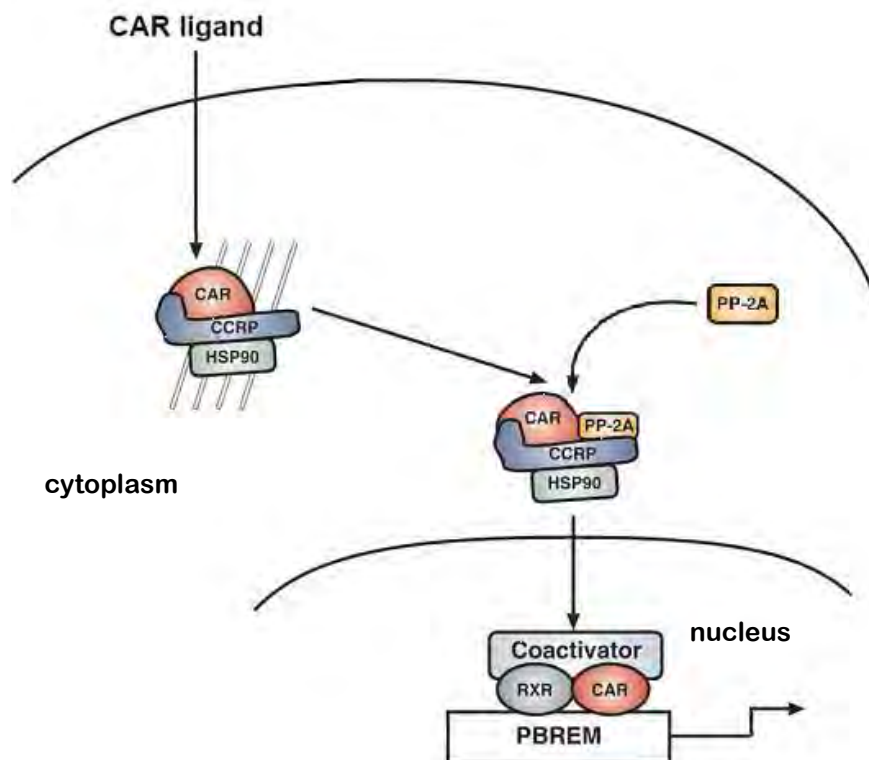


Figure 6 Mechanism of CYP2C9 gene transcription activation (Swales and Negishi, 2004)

4.2.3 CYP3A induction

This CYP exhibits very broad specificity and is induced by a structurally diverse group of substances. Induction mechanism is activated by binding of ligand to pregnane X receptor (PXR). The inducers possess a highly flexible recognition site which only requires a very poor substrate fitting for activation to occur. Thereafter, it binds to retinoic acid X receptor (RXR) then binds to ER6 elements that are upstream of the CYP3A4 gene (Figure 7) (Hukkanen, 2000).

Pharmaceuticals activating PXR include steroids, macrolide antibiotics, rifampicin, phenobarbital, barbiturates and even pesticides (Coleman, 2005).

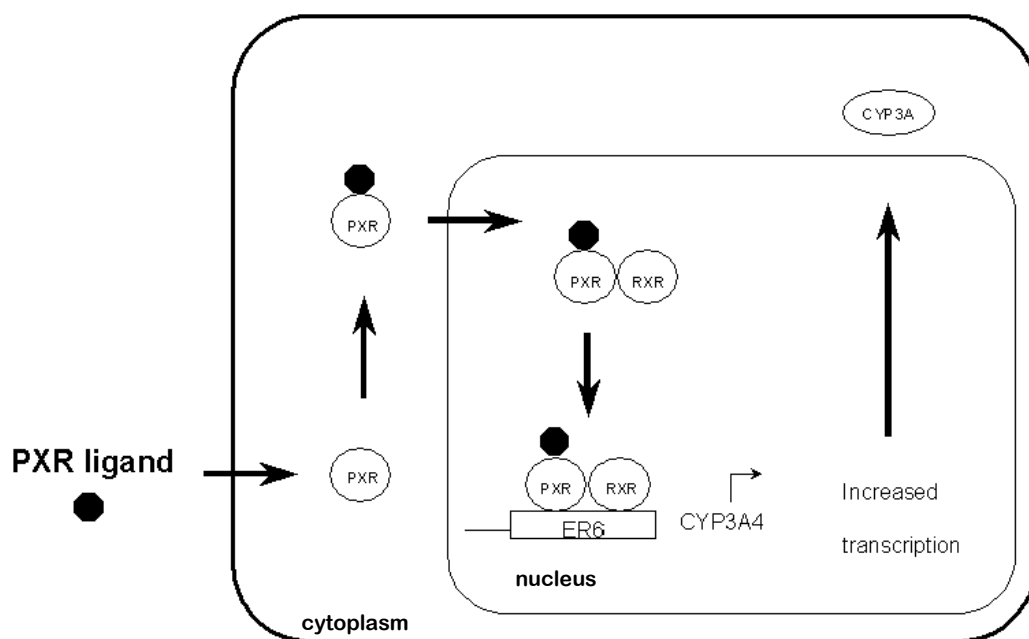


Figure 7 Mechanism of CYP3A4 gene transcription activation (Hukkanen, 2000)

4.2.4 CYP2E1 induction

CYP2E1 is induced by small hydrophilic molecules such as ethanol, acetone and pyridine as well as by systemic stress such as diabetes and starvation. Unlike others, transcriptional regulation seems to play a minor role in the induction of CYP2E1. For instance, the induction of CYP2E1 protein by ethanol involved in an increase in protein synthesis or stimulation of translation and steady-state of CYP2E1 mRNA rather than decrease in CYP2E1 degradation (Tsutsumi, Lasker, and Takahashi, 1993).

Since, many studies supported that AuNPs were able to enter into cells, they may influence on the amount of CYPs by induction or decrease the expression of CYP mRNAs which will be discussed in next sections.

CHAPTER III

MATERIALS AND METHODS

1. Materials

1.1 Equipment

- | | |
|--|---------------------------|
| 1. -20°C deep freezer | Hitachi, Japan |
| 2. Refrigerator | Sharp, Japan |
| 3. 24-well plate | Costar, USA |
| 4. Autoclave | Sturdy Industrial, Taiwan |
| 5. Cell culture flask 25 cm ² | TPP, Switzerland |
| 6. Counting chamber | Beeco, Germany |
| 7. De-ionized water
(DI water) system | ELGA, England |
| 8. Disposable pipette 5 mL | Costar, USA |
| 9. DNA thermal cycler | Biometra, Germany |
| 10. Gel document: Gel Doc TM | Bio-Rad, USA |
| 11. Gel electrophoresis | Toyobo, Japan |
| 12. Incubator | Thermo Scientific, USA |
| 13. Lamina flow | BossTech, Thailand |
| 14. Light microscope | Nikon, Japan |
| 15. Magnetic stirrer | Clifton, USA |
| 16. Microcentrifuge : Minispin | Eppendorf, Germany |
| 17. Microcentrifuge tube (200 µL
and 1.5 mL RNase/DNase free) | Corning, USA |

- | | |
|---|-------------------------------------|
| 18. Micropipettes SL-20 (2-20 μ L),
SL-200 (20-200 μ L) and
SL-1000 (100-1,000 μ L) | Rainin, USA |
| 19. Micropipettes tips
(RNase/DNase Free) | Corning, USA |
| 20. Microplate reader | PerkinElmer, USA |
| 21. PCR 96-well plate | Axygen Scientific, USA |
| 22. Pipette controller | Brand Tech, USA |
| 23. Real-time PCR machine:
ABI PRISM [®] 7700 | Applied Biosystem, USA |
| 24. Stirrer hot plate | BEC Thai, Thailand |
| 25. Timer | Citizen, Japan |
| 26. Transmission Electron
Microscopy: JEM-2100 | Jeol, Japan |
| 27. Ultracentrifugal filter 3 kDa | Millipore, USA |
| 28. UV-visible spectrophotometer | Thermo Scientific /
BioMate, USA |
| 29. Vortex mixer | Clay Adams, USA |
| 30. Water bath | Thelco, USA |
| 31. Zetasizer NanoZS | Malvern, UK |

1.2 Chemicals

- | | |
|----------------------|-------------------|
| 1. 100 bp DNA ladder | NEB, UK |
| 2. 100 mM dNTP mix | Fermentas, Canada |

3. 6X loading dye solution Fermentas, Canada
4. Absolute ethanol Lab Chem, Thailand
5. Agarose Research Organics Inc., USA
6. Alpha-naphthoflavone Sigma-Aldrich, USA
(C₁₉H₁₂O₂, MW = 272.3)
7. Dimethylsulfoxide (DMSO) Sigma-Aldrich, USA
8. Distilled water Invitrogen, USA
(DNAse, RNAse free)
9. Dulbecco's modified Invitrogen, USA
Eagle's medium (DMEM)
10. DyNAmo™ qPCR kit Finnzymes, Finland
11. Ethidium bromide Sigma-Aldrich, USA
12. Fetal bovine serum (FBS) Invitrogen, USA
13. HotStarTaq DNA polymerase Qiagen, USA
14. Hydrogen tetrachloroaurate Sigma-Aldrich, USA
(III) trihydrate (MW = 393.83)
15. L-glutamine Invitrogen, USA
16. 3-(4,5-dimethylthiazol-2-yl)-2, Sigma-Aldrich, USA
5-diphenyltetrazolium bromide (MTT)
17. Penicillin/streptomycin Invitrogen, USA
18. Polyethyleneimine Sigma-Aldrich, USA
(MW ~ 750 kDa)
19. RevertAid™ first strand Fermentas, Canada
cDNA synthesis kit

20. Rifampicin	Siam Pharmaceutical, Thailand
21. Total RNA mini kit	Geneaid, Taiwan
22. Tris base	Research Organics Inc., USA
23. Trisodium citrate dihydrate (MW = 37.83)	Sigma-Aldrich, USA
24. Trypsin	Invitrogen, USA
25. Tryptan blue stain 0.4%	Invitrogen, USA
26. Ultrapure water (18.2 M Ω)	Elga, UK

2. Methods

2.1 Preparation of gold nanoparticles

Gold nanoparticles (AuNPs) at a concentration of 1,015 μM (200 ppm) were prepared according to Turkevich method (Kimling *et al.*, 2006) using citrate and polyethyleneimine (PEI) as stabilizers. Glassware were cleansed with aqua regia ($\text{HCl}:\text{HNO}_3 = 3:1$) for the purpose of circumventing gold contamination, and rinsed with ultrapure water and oven dried prior to use.

Gold nanoparticles were synthesized using citrate as a stabilizer in 3 conditions. Firstly, 35 μL of 30% hydrogen tetrachloroaurate (III) trihydrate ($\text{HAuCl}_4 \cdot 3\text{H}_2\text{O}$) was added to 49.5, 49 or 48 mL ultrapure water for conditions 1, 2 and 3, respectively. The sample was then heated up to 90°C in a water bath with stirring. Next, 0.5 (condition 1), 1 (condition 2) or 2 (condition 3) mL of 0.4 M trisodium citrate dihydrate ($\text{Na}_3\text{C}_6\text{H}_5\text{O}_7 \cdot 2\text{H}_2\text{O}$) were added to the gold solution flask and continued heating until it became dark red. Gold nanoparticles were then stored at $3\text{-}5^\circ\text{C}$ in a light-protected container. Preparation process of citrate-stabilized AuNPs (AuCi) is shown in Figure 8.

The same procedure was applied to prepare AuNPs stabilized by polyethyleneimine (PEI, $-(\text{CH}_2\text{CH}_2\text{NH})_n-$) in which 0.5, 1 or 2 mL of 0.036 M PEI solution was used instead of the citrate solution for conditions 1, 2 and 3, respectively. The formation of AuNPs proceeded first as orange color and finally dark red. The step for synthesis of polyethyleneimine stabilized AuNPs (AuPEI) is shown in Figure 9. Prior to cell culture test, excess amount of stabilizer were removed by using 3 kDa ultra centrifugal filter (5000 x g, 20 min) twice.

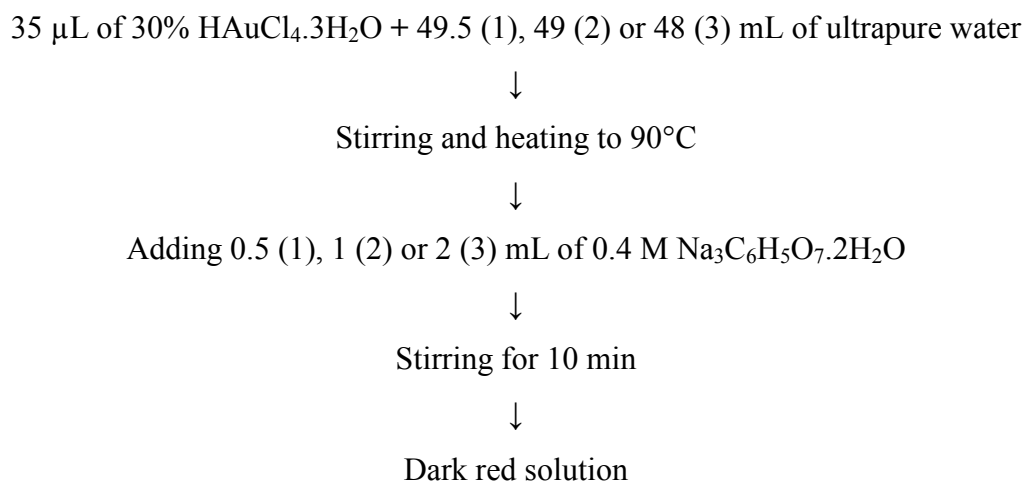


Figure 8 Synthesis of citrate stabilized gold nanoparticles (Kimling *et al.*, 2006) with 3 different conditions as indicated in bracelets

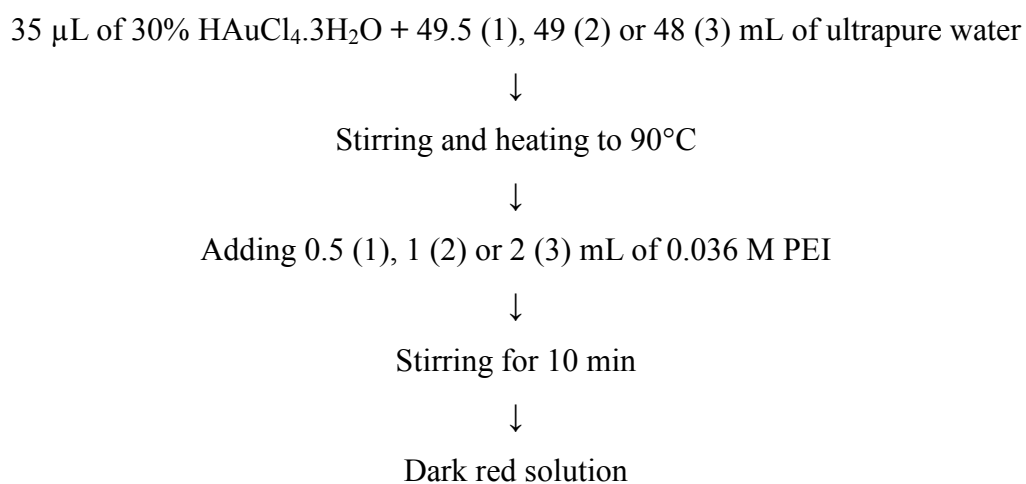


Figure 9 Synthesis of polyethyleneimine stabilized gold nanoparticles (Kimling *et al.*, 2006) with 3 different conditions as indicated in bracelets

2.2 Characterization of gold nanoparticles

The absorbance profiles of AuNPs were characterized by using UV-visible spectroscopy. Zeta potential measurement of AuNPs was performed with Zetasizer NanoZS and particle size and morphology of the nanoparticles were observed under Transmission Electron Microscopy (TEM) (Jeol, Japan). The characterizations of AuNPs were carried out after synthesis and after one month storage.

2.2.1 UV-visible spectroscopy

AuNPs were observed under UV-visible spectroscopy to obtain optical spectra. The machine was set to use a Xenon lamp in a single beam within the range of 400-700 nm. Ultrapure water was used as a reference standard to set a basal line before measurement. The experiment performed using a UV quartz cuvette with a path length of 10 nm as a container. The observed spectra are related to an excitation of surface plasmon resonance (SPR). This phenomenon occurs when there are collective oscillations of electrons at the metallic nanoparticles-dielectric medium interface which correspond to a light source. The SPR makes surface plasmon band which generates the color appearance of the nanoparticles. The peak wavelength (λ_{\max}) depends on size, shape, material and dielectric environment of the sample (Yonzon, Zhang and Van Duyne, 2003). Relationship between absorbance and size of spherical AuNPs was presented as the following equation (Khlebtsov, 2008):

$$\begin{aligned}
 d &= 3 + [(7.5 \times 10^{-5}) X^4] && \text{for } X < 23 \\
 d &= [\sqrt{X - 17} - 1] / 0.06 && \text{for } X \geq 23
 \end{aligned}
 \tag{2}$$

where, d = diameter of the sphere (nm), when $5 \leq d \leq 100$

X = maximum absorbance wavelength (λ_{\max}) – 500

An increase in particle diameter gives an increase in maximum absorbance wavelength (λ_{\max}) and gives more purple color (Murphy *et al.*, 2008). Spherical gold nanoparticles in the diameter of 10-40 nm generate red color when non-spherical or bigger sizes of gold nanoparticles generate blue color (Haiss *et al.*, 2007; Kimling *et al.*, 2006; Murphy *et al.*, 2008).

2.2.2 Zeta potential measurement

The zeta potential of AuNPs was measured with Zetasizer NanoZS (Malvern, UK). The zeta potential provides information of surface charge of the nanoparticles by using laser Doppler electrophoresis technology which may be related to colloidal stability due to electrostatic force between particles (Note, Kosmella and Koetz, 2006). The particles are accelerated by giving an electric field to move and change the frequency. With the light source, altering scattered light gives a modulated signal (electrophoretic mobility, U_E) which can be calculated for the zeta potential by using the following Henry's equation (Sjöblom, 2006):

$$U_E = \frac{2 \varepsilon \zeta f(\kappa a)}{3 \eta} \quad (3)$$

where, ζ = zeta potential (mV)
 ε = dielectric constant (Farads per meter; F/m)
 η = viscosity (Pascal second; Pa s)
 $f(\kappa a)$ = Henry's function

2.2.3 Size and size distribution

The TEM technique was used for illustrating physical shape and size of the AuNPs. Ten microliters of the synthesized AuNPs was dropped into a carbon-coated 200-mesh copper grid and let it air-dried overnight before taken pictures under TEM. SemAfore digitizer program (JEOL, Sweden) was used to obtain size and size distribution.

2.3 Cell line and cell culture

The human liver cell line HepG2 (hepatocellular carcinoma) were obtained from American Type Culture Collection (ATCC) and cultured in Dulbecco's modified Eagle's medium (DMEM) with 10% (v/v) fetal bovine serum, 2 mM L-glutamine and antibiotics (50 μ g/mL penicillin, 50 μ g/mL streptomycin). Cultures were maintained in an atmosphere with 5% CO₂ at 37°C and medium was refreshed every three or four days with subculturing (Maruyama *et al.*, 2007).

2.4 Cytotoxicity test of gold nanoparticles

Evaluation of cytotoxicity was performed using the 3-(4,5-dimethylthiazol-2-yl)-2,5-diphenyltetrazolium bromide (MTT) tetrazolium assay to obtain concentration of AuNPs for further experiment.

HepG2 cells were seeded in 96-well tissue culture plate at a density of 2×10^4 cells/well in 100 μL of assay medium and incubated overnight at 37°C under 5% CO_2 atmosphere. The cells were then treated with 10 μL of AuNPs at concentrations of Au atom ranging from 0.1 to 90 μM ($n = 8$ for each concentration) and incubated for 48 h. The cells grown in medium were used as a control. Then, the cells were washed with 100 μL of PBS and refreshed with 100 μL of medium. Two microliters of 2% MTT in dimethyl sulfoxide (DMSO) was added to each well and incubated the plate at 37°C for 4 h. The assay measured the enzymatic reduction of dehydrogenase enzyme in the living cell which results in a change of yellow tetrazolium MTT to purple formazan crystal (Levitz and Diamond, 1985). Then, 100 μL of DMSO was added to dissolve the formazan crystal. The plate was shaken at high intensity for 30 sec before measuring the absorbance at 570 nm with 620 nm as a reference wavelength using a microplate reader (PerkinElmer, USA). Cell viability was calculated as the following equation:

$$\% \text{Viability} = \frac{\text{Optical density unit of treated sample}}{\text{Optical density unit of control}} \times 100 \quad (4)$$

The concentrations with more than 90% cell viability were considered as non-toxic doses and were used to investigate the effect of AuNPs on CYP gene expression. Values of IC_{50} (the concentration with 50% viability) were also

calculated using GraphPad Prism 4.03 program (San Diego, USA) with an equation for sigmoidal dose-response to generate non-linear regression curves.

2.5 Detection of CYP gene in HepG2 cell line

HepG2 cell line was determined for CYP1A1, CYP1A2, CYP2C9, CYP2E1 and CYP3A4 to ensure the exhibition of CYPs in the cells. The PCR conditions were also tested before performing in a real-time PCR machine.

2.5.1 RNA extraction

Total RNA was extracted from HepG2 cells using total RNA mini kit (Geneaid[®], Taiwan). Equipments and chemicals used within contact with cells were all ribonuclease (RNase) free until the RNA has successfully converted to cDNA in the further section. According to the manufacturer's instruction, the 3×10^6 cells were transferred to a 1.5-mL microcentrifuge tube and the cells were centrifuged at 8,000 rpm for 20 sec. Then, the supernatant was completely removed and the cells were suspended in 100 μ L of PBS. Afterwards, the cells were lysed by adding 400 μ L of lysis buffer (RB Buffer[®]) and vortexed. The cell suspension was incubated at room temperature for 5 min. Then, 400 μ L of 70% ethanol was added to the lysed cell and the suspension was mixed immediately by pipetting. The mixture was thereafter transferred to a column containing silica filter, placed in a 2-mL collection tube, and centrifuged at 13,000 rpm for 2 min. Four hundred microliters of W1 Buffer[®] was added into the column and centrifuged at 13,000 rpm for 1 min. Next, 600 μ L of washing buffer was added into the column and centrifuged at the same speed for 1 min. Finally, the dried column was placed in a RNase-free 1.5-mL microcentrifuge tube with an addition of 50 μ L of RNase-free water into the center of the column

matrix. After 3 min, the tube was centrifuged at 13,000 rpm for 1 min to elude the purified RNA.

Total RNA concentration was measured using UV-visible spectrophotometer (BioMate, Thermo Fisher Scientific, USA) with RNase-free water for setting a zero base line. The absorbance at 260 nm was used to calculate for RNA concentration for further use as a template for synthesis of cDNA. RNA could be kept at -20°C before the conversion to cDNA for a few days.

2.5.2 Synthesis of cDNA

RevertAid™ first strand cDNA synthesis kit (Fermentas®, Lithuania) was used for synthesis of cDNA according to the manufacturer's instruction. First, oligo dT 1 µL (0.5 µg) was added into 5 µg of RNA dissolved in 11 µL of diethylpyrocarbonate (DEPC) treated water. The mixture was then incubated at 70°C for 5 min. Thereafter, the mixture was added with 4 µL of 5X reaction buffer, 1 µL of ribonuclease inhibitor (20 U/µL), 2 µL of 10 mM nucleotides (dNTP), and 1 µL of reverse transcriptase (200 U/µL), respectively. The mixture was mixed, spun down, and incubated at 42.0°C for 60 min and 70.0°C for next 10 min. The synthesized cDNA was kept at -20°C for using as a template for polymerase chain reaction (PCR) method.

2.5.3 Gene expression assay

2.5.3.1 Primer selection

In order to investigate the gene expression, the specific primers of both forward and reverse sequences were needed in the reverse transcriptase polymerase chain reaction (RT-PCR) method to amplify the amount of mRNA. The CYP1A1,

CYP1A2, CYP2C9, CYP2E1, CYP 3A4 and GAPDH primers from human mRNA sequences were chosen from experiments in which the sequences were confirmed via NCBI (National Center for Biotechnology Information, USA) and Ensembl (UK) blast search to ensure the correct targeted mRNA (Haas *et al.*, 2005; Rodriguez-Antona *et al.*, 2001; Westerink and Schoonen, 2007). The primers were selected based on melting temperature at around 60°C for the simply setting of annealing temperature. In addition each primer pair had to bind to the different exons for more specificity. GAPDH was used as a reference gene (house-keeping gene). Forward and reverse primer sequences for all CYPs and GAPDH along with their PCR product lengths are shown in Table 2. The primers were kept in 200 µM stock solution at -20°C. The stock solution was diluted to obtain a working formula at the concentration of 20 µM prior to use.

Table 2 Primer sequences for CYP1A1, CYP1A2, CYP2C9, CYP2E1, CYP3A4 and GAPDH. (Haas *et al*, 2005; Westerink and Schoonen, 2007)

Gene	Primer	PCR product length (base pair)
CYP1A1	Forward: 5' TCG GGG AGG TGG TTG GCT CT 3' Reverse: 5' TGT CCC GGA TGT GGC CCT TCT 3'	171
CYP1A2	Forward: 5' GGA GCA GGA TTT GAC ACA GTC A 3' Reverse : 5' GCT CCT TCT GGA TCT TCC TCT GTA 3'	94
CYP2C9	Forward: 5' TTC AGT CCT TTC TCA GCA GG 3' Reverse : 5' TTG CAC AGT GAA ACA TAG GA 3'	383
CYP2E1	Forward: 5' GTG GAG GCA GGT GCA CAG CA 3' Reverse: 5' TGG GCC AAC CGG GTG AAG GA 3'	117
CYP3A4	Forward: 5' CAG GAG GAA ATT GAT GCA GTT TT 3' Reverse: 5' GTC AAG ATA CTC CAT CTG TAG CAC AGT 3'	78
GAPDH	Forward: 5' CCA TGG CAC CGT CAA GGC TGA 3' Reverse : 5' CTC CAT GGT GGT GAA GAC GC 3'	151

2.5.3.2 Polymerase chain reaction (PCR)

Gradient PCR machine (Mastercycler gradient, Eppendorf, German) was used to determine the optimum annealing temperature. In order to avoid DNA contamination, apparatus and chemicals used were separated from other experiments. Amplification of cDNA was performed using cDNA equivalent to 500 ng of total RNA for the analysis of CYP gene expression. The total mixture containing 2 μ L of cDNA, 0.2 μ M of forward primer, 0.2 μ M of reverse primer, 0.2 μ M of dNTP, 1X PCR buffer, 0.25 U of HotStarTaq DNA polymerase enzyme (Qiagen, USA), was adjusted the final volume of 10 μ L using purified water. For the negative control tube, cDNA was substituted with purified water. Four sets of the each primer pair

were performed with four different annealing temperatures, 60.0, 58.8, 56.2 and 54.0°C. The condition used for cDNA amplification was set for gradient program: 95.0°C for 5 min, 40 cycles of 95.0°C for 1 min (denature), four different annealing temperatures for 1 min, and 72.0°C for 1 min (extension) and to end with 72.0°C for 5 min. The amplified products were kept at 4.0°C prior to use.

2.5.3.3 Gel electrophoresis

The gel electrophoresis was used to investigate amplified PCR products using electric current to drive DNA from negative to positive electrode through gel matrix.

2.5.3.3.1 Gel preparation

Firstly, 800 mg of agarose was dissolved in 40 mL of Tris-boric EDTA (TBE) buffer with an addition of heat for about 1 min or until the solution was clear. When the solution stopped boiling and started to cool down, 3 µL of 0.1% ethidium bromide was added into to gel solution and stirred. The settle plate was also needed to check with a bubble clinometer whether it was in planar before pour the gel solution into a settle plate with a comb to make several wells at one side. The gel should not have any bubble inside which could be a great barrier of DNA pathway. The gel was then left until it was set.

2.5.3.3.2 Electrophoresis

The firmed gel was moved into an electrophoresis apparatus under 1X TBE buffer. The well part should be at the negative pole (anode) since the DNA will go to the positive pole (cathode). Either 10 µL of the RT-PCR product or 2 µL 100 bp DNA ladder (New England Biolabs, UK) was mixed with 3 µL of loading dye, bromphenol blue before putting on wells in the gel. The machine was turned on and

set at approximately 100 mV for about 1 h. Larger DNA molecule could run through the gel matrix slower than smaller ones. The gel was investigated under UV light using GelDocTM (Bio-Rad, USA) machine. Ethidium bromide can fluoresce orange color under UV light at almost 20 fold when intercalated into DNA minor groove.

2.6 Investigation of AuNPs influence on CYP mRNA expression

2.6.1 Treatment of cultures

The cells were seeded approximately 1×10^6 cells per 25-cm² flask and grown in DMEM medium under the atmosphere of 5% CO₂ at 37°C for 24 h. Thereafter, the cells were incubated with 1 or 10 μM of AuCi and 0.1 or 1 μM of AuPEI in the medium or incubated with only medium (control) for 48 h. The cells were also incubated with the specific inducers for each CYP. The α-naphthoflavone (αNF) was used at 10 μM as CYP1A1 and CYP1A2 inducers, ethanol (EtOH) was used at 500 mM as CYP2E1 inducer while rifampicin (Rif) was an inducer for CYP2C9 and CYP3A4 and used at a concentration of 10 μM (Alexandre *et al.*, 1999; Ishida *et al.*, 2002; Trubetskoy *et al.*, 2004; Westerink and Schoonen, 2007). In addition, the effect of DMSO as a solvent for αNF and Rif was also studied on CYP expressions.

2.6.2 RNA extraction

The treated cells were extracted for RNA by the same method as previously described in section 2.5.1.

2.6.3 Gene expression assay

The obtained RNA from section 2.6.2 was used as templates for cDNA synthesis by the same procedure as described in section 2.5.2. The cDNA was subjected to amplification by real-time PCR machine using the proposed primers (in section 2.5.3.1) and calculated for fold of induction using $2^{-\Delta\Delta C_t}$ method (Livak and Schmittgen, 2001).

2.6.3.1 Amplification with real-time performance

Effects of AuNPs on CYPs expression were examined using real-time RT-PCR technique and analyzed by ABI PRISM[®] 7700 sequence detection system (Applied Biosystem, USA). The total mixture composed of 1 μ L of cDNA, 0.1 μ M of forward primer, 0.1 μ M of reverse primer, 0.3X ROX (6-carboxyl-X-rhodamine) reference dye, 1X SYBR PCR master mix (Finnzymes[®], Finland) was adjusted the total volume to 20 μ L per reaction using purified water. Negative control was included as the same condition with the substitution of cDNA with purified water at the same amount for the detection of contamination. The PCR condition was set according to the manufacturer's suggestion as: 95.0°C for 10 min and 50 cycles of 95.0°C 15 sec, 60.0°C 20 sec and 72.0°C 40 sec.

2.6.3.2 Data analysis with $2^{-\Delta\Delta C_t}$ method

Expression levels were normalized with the GAPDH gene then compared with control using real-time quantitative PCR and the $2^{-\Delta\Delta C_t}$ method (Livak and Schmittgen, 2001). After the cycle threshold value provided from real-time PCR instrument, fold induction can be calculated as the following equation:

$$\text{Fold induction} = 2^{-\Delta\Delta C_t} \quad (5)$$

where, $\Delta\Delta C_t = (C_{t,GAPDH} - C_{t,target})_{\text{control condition}} - (C_{t,GAPDH} - C_{t,target})_{\text{treated condition}}$

$C_{t,GAPDH}$ = cycle threshold of GAPDH

$C_{t,target}$ = cycle threshold of target

Control condition = the condition of cells treated with medium only

2.7 Statistical analysis

The value of IC_{50} obtained from toxicity assay were compared using unpaired student's t test. The gene expression results were analyzed using one-way analysis of variance (ANOVA) with Bonferroni post hoc test in order to determine significant differences among fold inductions ($p \leq 0.05$).

CHAPTER IV

RESULTS AND DISCUSSION

1. Characterization of gold nanoparticles

1.1 Appearances

The reduction of gold from Au^{3+} to Au^0 was used for the preparation of AuNPs. Trisodium citrate dihydrate ($\text{Na}_3\text{C}_6\text{H}_5\text{O}_7 \cdot 2\text{H}_2\text{O}$) and polyethyleneimine (PEI, $-(\text{CH}_2\text{CH}_2\text{NH})_n-$) were used as reducing and stabilizing agents. AuCi were prepared using various molar ratios of gold atom (Au) to trisodium citrate, 1:4 (condition 1), 1:8 (condition 2) and 1:16 (condition 3) while the molar ratios of Au to PEI at 1:0.35 (condition 1), 1:0.7 (condition 2) and 1:1.4 (condition 3) were used for AuPEI preparation. The appearances of citrate-stabilized gold nanoparticles (AuCi) and PEI-stabilized gold nanoparticles (AuPEI) after synthesis and one month storage were illustrated in Figure 10.

Kimling *et al.* (2006) performed AuCi at a molar ratio of Au to trisodium citrate at around 1:8. This ratio was the same as in condition 2 which was expected to be the suitable concentration. From the results, citrate-stabilized gold nanoparticles after synthesis using conditions 1 and 2 were red but those using condition 3 looked rather purple, which was in an agreement with Kimling *et al.* (2006). After one month of storage, the color of AuNPs (condition 3) changed to be light purple with small dark particles floating and precipitating at the bottom. In addition, some of small dark particles were found floating on top of the AuNPs prepared using condition 2. The transformation of color from red to purple indicated an increase in

particle sizes (Murphy *et al.*, 2008). Thus, the most suitable concentration ratio of Au to trisodium citrate dihydrate was 1:4 (condition 1).

The stable condition of AuPEI had presented by Sun *et al.* (2003) in that the molar ratio of Au to PEI was 1:0.68 which was used in condition 2 (1:0.7). Appearances of AuNPs stabilized by PEI after synthesis and one month storage looked very similar. However, condition 3 appeared to be rather purple than the others. These results implied that concentration ratios of Au to PEI of 1:0.35 and 1:0.7 (conditions 1 and 2) could produce more stable PEI-stabilized AuNPs.

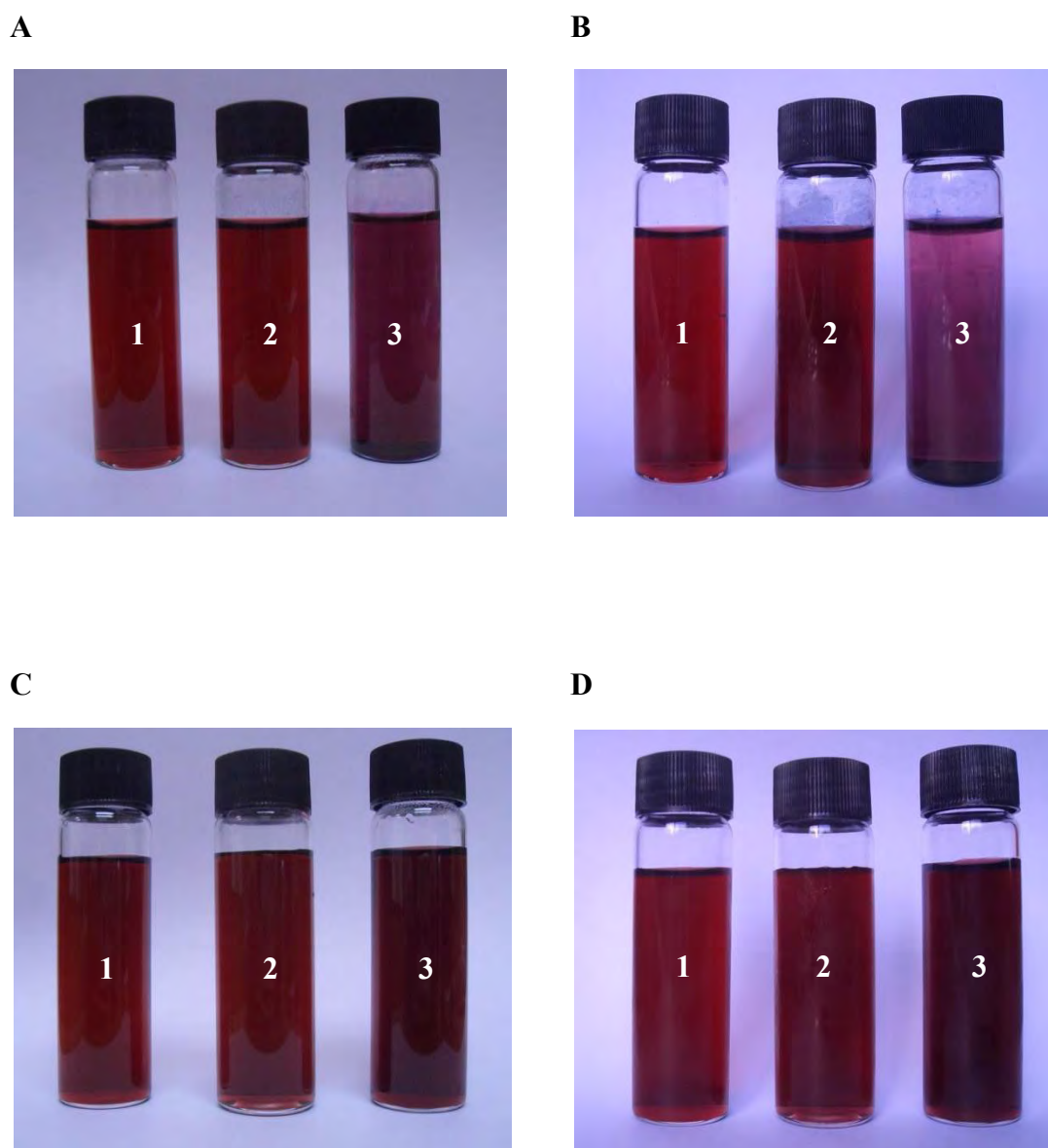


Figure 10 The appearances of citrate-stabilized AuNPs after synthesis (A) and 1 month storage (B), PEI-stabilized AuNPs after synthesis (C) and 1 month storage (D), prepared using conditions 1, 2 and 3.

1.2 UV-visible spectroscopy

Both AuCi and AuPEI prepared from each condition were characterized for SPR characteristics as displayed in Figures 11-16. AuCi prepared using conditions 1 and 2 showed peaks of absorption wavelength (λ_{\max}) within the range of 520-523 nm both after synthesis and 1 month storage while the peaks of AuCi in condition 3 were found at 531 and 537 nm after synthesis and storage for a month, respectively. Furthermore, an absorbance of AuCi in condition 3 was noticeably lower than those in other conditions and dramatically decreased after 1 month storage. The λ_{\max} of AuPEI in conditions 1 and 2 were discovered between 513-516 nm after synthesis and time storage. Peak of absorption of AuPEI prepared with condition 3 was found at 522 nm after synthesis and shifted to 524 nm after 1 month storage.

The absorption peaks were associated with the size of particles and their concentrations (Baptista *et al.*, 2007; Haiss *et al.*, 2007). The higher wavelength of absorbance peak (λ_{\max}) may indicate the larger size while the higher absorbance may indicate the higher nanoparticle concentration (Daniel and Astruc, 2004; Khlebtsov, 2008; Song *et al.*, 2009). Thus, AuCi conditions 1 and 2 seemed to be very stable. On the other hand, AuCi condition 3 which were noticeably decreased in the absorbance and the shift to longer λ_{\max} pointed to instability of nanoparticles in which precipitation of AuNPs was found. Peaks of absorption for AuPEI in condition 1 after storage were similar to those after synthesis while there were some small changes in the absorbances of AuPEI in conditions 2 and 3 after storage which implied that condition 1 seemed to be the most stable for nanoparticle preparation.

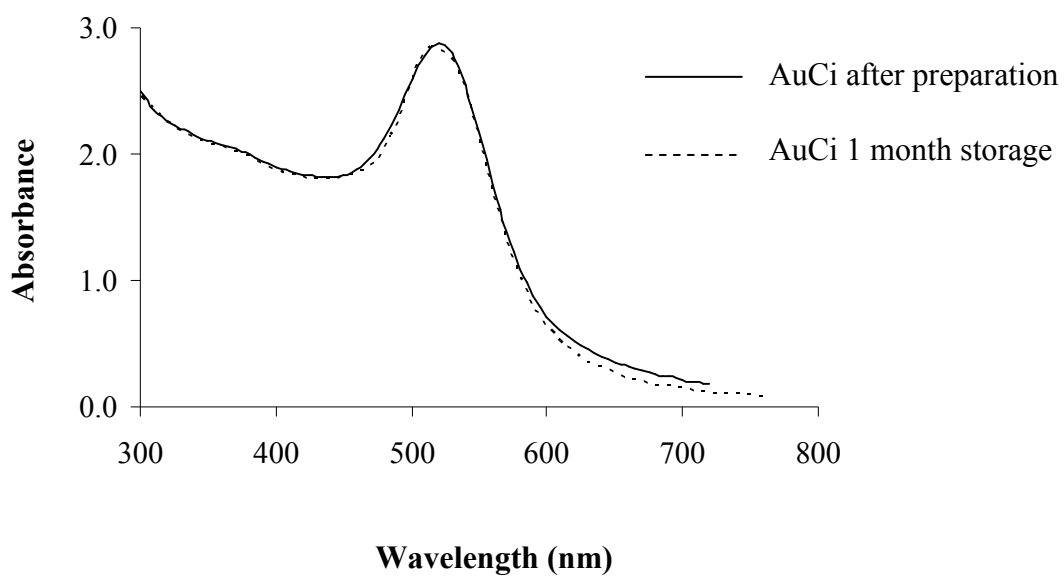


Figure 11 UV absorption spectra of citrate-stabilized AuNPs prepared with condition 1 after preparation and 1 month storage

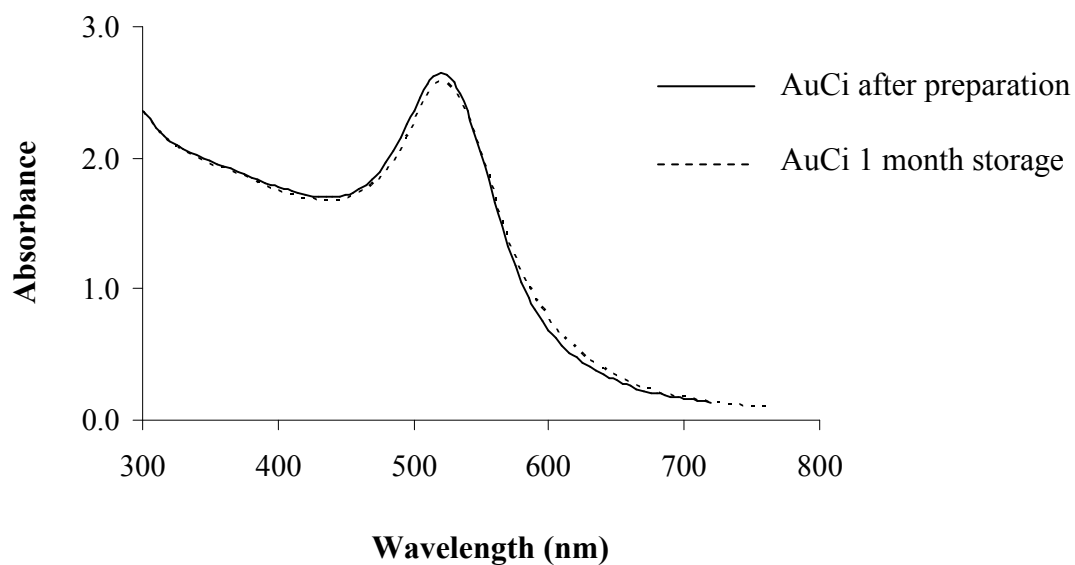


Figure 12 UV absorption spectra of citrate-stabilized AuNPs prepared with condition 2 after preparation and 1 month storage

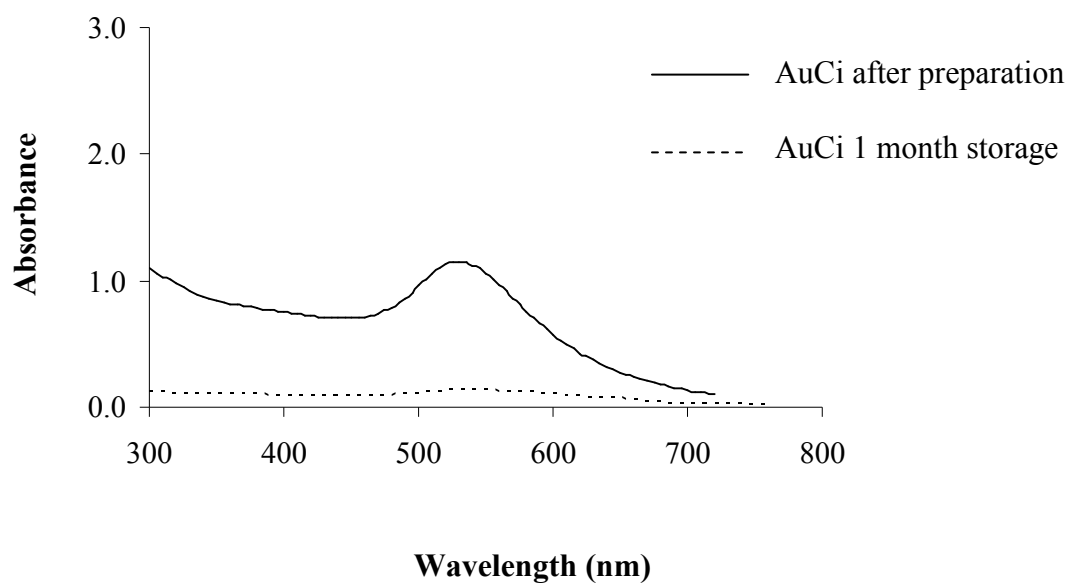


Figure 13 UV absorption spectra of citrate-stabilized AuNPs prepared with condition 3 after preparation and 1 month storage

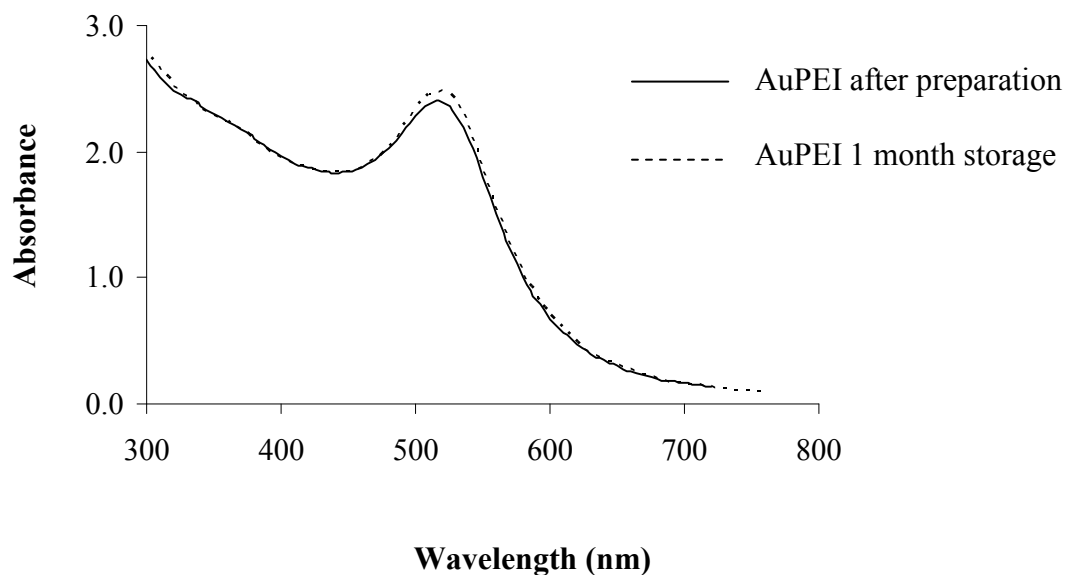


Figure 14 UV absorption spectra of PEI-stabilized AuNPs prepared with condition 1 after preparation and 1 month storage

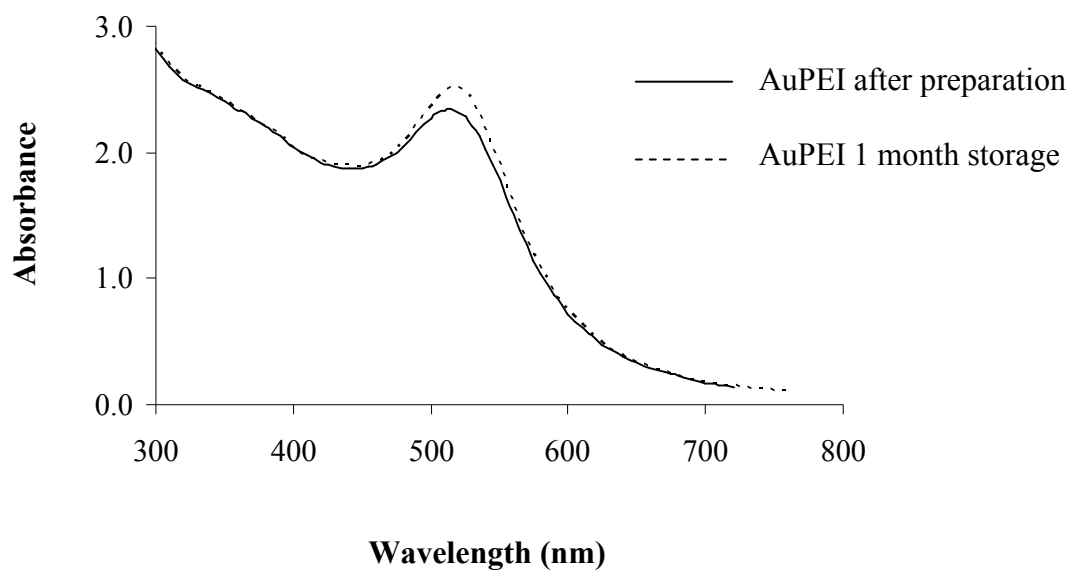


Figure 15 UV absorption spectra of PEI-stabilized AuNPs prepared with condition 2 after preparation and 1 month storage

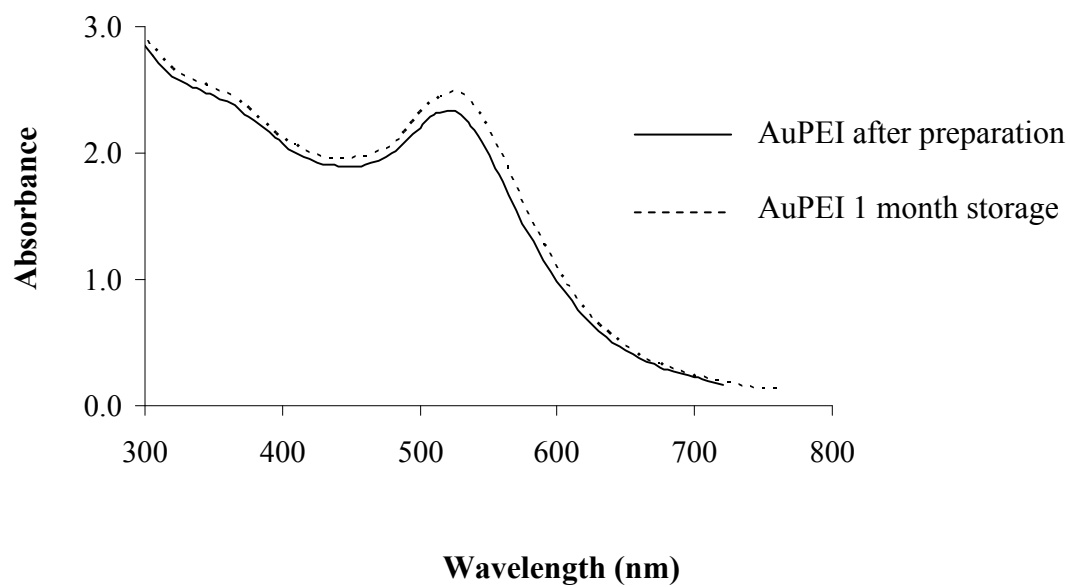


Figure 16 UV absorption spectra of PEI-stabilized AuNPs prepared with condition 3 after preparation and 1 month storage

1.3 Zeta potential measurement

AuNPs were determined for their surface charges by Zetasizer NanoZS. From the results, AuCi prepared using conditions 1, 2 and 3 illustrated negative charges of -40.60 ± 1.22 , -20.20 ± 2.11 , and -38.80 ± 5.16 mV, respectively while the positive charges of 8.10 ± 1.59 , 19.90 ± 1.40 , and 15.60 ± 2.32 mV were obtained from AuPEI prepared using conditions 1, 2 and 3, in orderly. There was a decrease in negative charges of AuCi in condition 1 after one month storage to -35.60 ± 0.25 mV while AuCi in condition 2 was found an increase in negative charges to -25.50 ± 4.20 mV. Noticeably, there was a considerable decrease in the negative charges of AuCi in condition 3 to -26.70 ± 0.42 mV. AuPEI in conditions 1 and 2 had a slight decrease in their positive charges to 6.50 ± 1.42 and 18.10 ± 3.21 mV, respectively whereas those in condition 3 showed a little increase in the charge to 15.90 ± 1.00 mV.

The charges of AuNPs were dependent on the stabilizers in which negative charges were from trisodium citrate and positive charges were from PEI (Goodman *et al.*, 2004; Kumar, Gandhi and Kumar, 2007). From the Derjaguin-Landau-Verwey-Overbeek (DLVO) theory, the stability of colloid was caused by a combination of van der Waals attractive and electrostatic repulsive forces (Hubbard, 2002). The larger electrostatic repulsion results from the higher potential at the surface. The instability of AuNPs was caused by a decrease in zeta potential as a function of time, thus diminishing the barrier of potential that maintains in suspension, permitting interaction among the nanoparticles and leading to the forming of flocculates (Zhou *et al.*, 2009). Suspensions with zeta potentials of more than 30 mV or -30 mV are considered stable (Gibson *et al.*, 2009). Thus, AuCi in conditions 1 and 3 might be considered to be the stable conditions. However, zeta potential of the AuCi in

condition 3 decreased dramatically to lower than -30 mV after one month of storage which indicated instability of the system. From the recent results, AuCi condition 3 was unstable due to the aggregation.

Although the measured zeta potential of AuPEIs were below 30 mV in all conditions, the solutions seemed to be stable even after a month of storage. The stability of the particles could result from the steric stabilization of polymer chain (Hubbard, 2002; Kronberg *et al.*, 1990) together with electrostatic repulsion. It was notably that the lesser amount of PEI than citrate was needed for AuNP preparation because it is polyelectrolytes which can combine both steric and electrostatic stabilization whereas citrate provides electrostatic stabilization alone (Sun *et al.*, 2003). In this study, AuPEI in condition 1 showed the least alteration in the absorbance after storage, thus AuPEI condition 1 were chosen for use in further experiments.

1.4 Size and size distribution

AuCi and AuPEI prepared using condition 1 (Au : trisodium citrate = 1 : 4 and Au : PEI = 1 : 0.35) were chosen to investigate their morphology by TEM. The images show the spherical shapes of AuCi and AuPEI as seen in Figures 17(A, B) and 18(A, B), consecutively. Average particle diameters of AuCi and AuPEI after preparation were found to be 15.00 ± 2.77 nm (n = 291) and 5.02 ± 1.81 nm (n = 445), respectively (Figure 19(A) and 20(A), in orderly). After one month storage, shape of the AuNPs were the same with partial agglomeration as seen in Figures 17(C, D) for AuCi and 18(C, D) for AuPEI. The sizes of AuNPs were slightly increased to $16.30 \pm$

3.16 nm (n = 151) for AuCi and 6.01 ± 1.51 nm (n = 322) for AuPEI after one month storage (Figures 19(B) and 20(B), in orderly).

When the maximum absorbance wavelength of AuCi condition 1 (520 nm) was put in the relationship between absorbance and size of spherical AuNPs (as described in section 2.2.1, chapter 3), the calculated diameter of the particles was 15.00 nm which confirmed the result from the TEM. The calculated diameter for AuPEI condition 1 was 5.14 nm which was very similar from the TEM result (5.02 ± 1.81 nm). The findings in this study were similar to other previous reports in that the AuNPs had the size of around 13-15 nm for AuCi (Pong *et al.*, 2007) and 4.7 ± 2.8 nm for AuPEI (Köth, Koetz and Appelhans, 2008). An increase in the particle sizes of the AuNPs may be due to a decrease in the inter-particle distance which brings to an agglomeration (Baptista *et al.*, 2007).

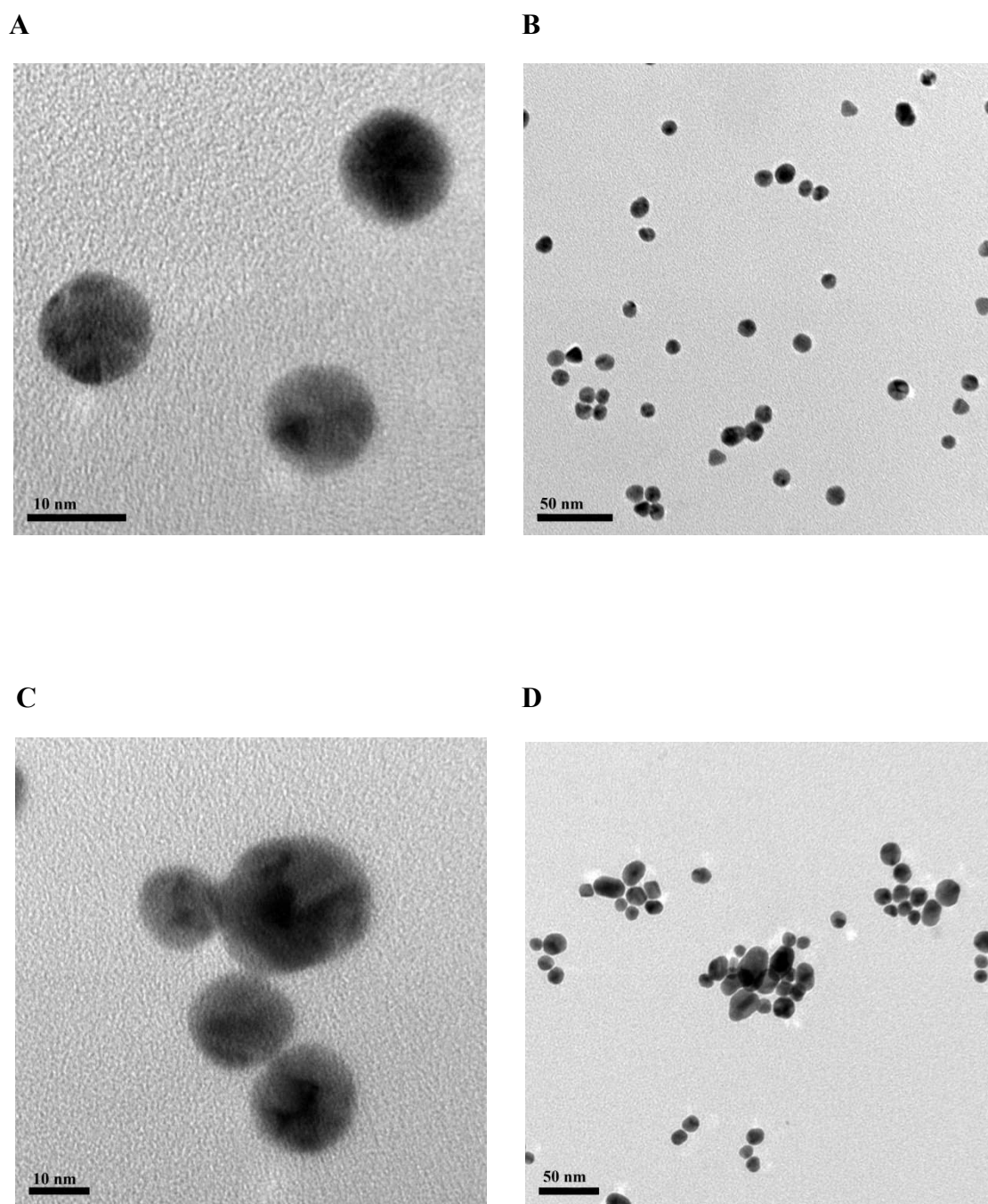


Figure 17 TEM images of citrate-stabilized AuNPs after preparation (A, B) and 1 month storage (C, D)

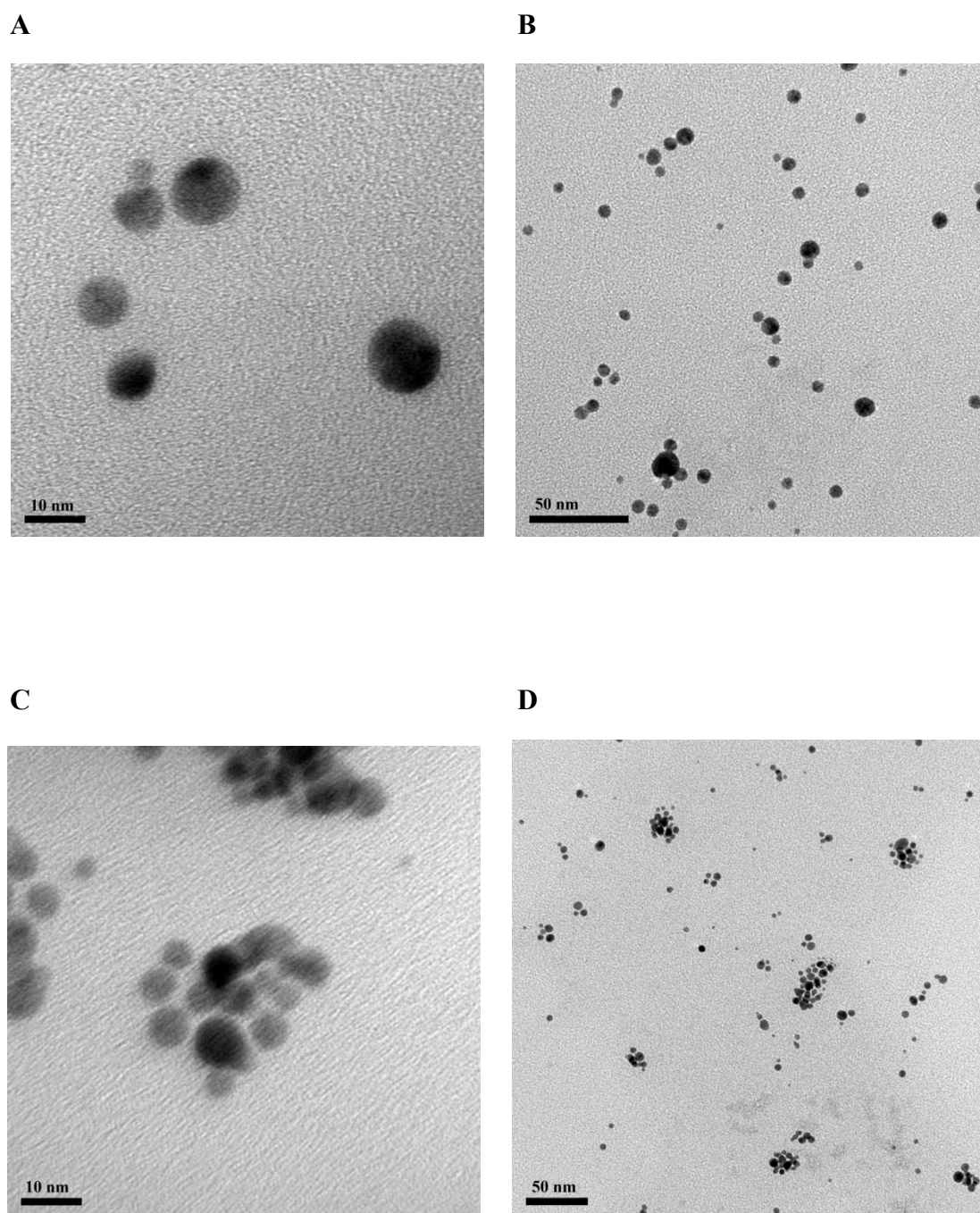
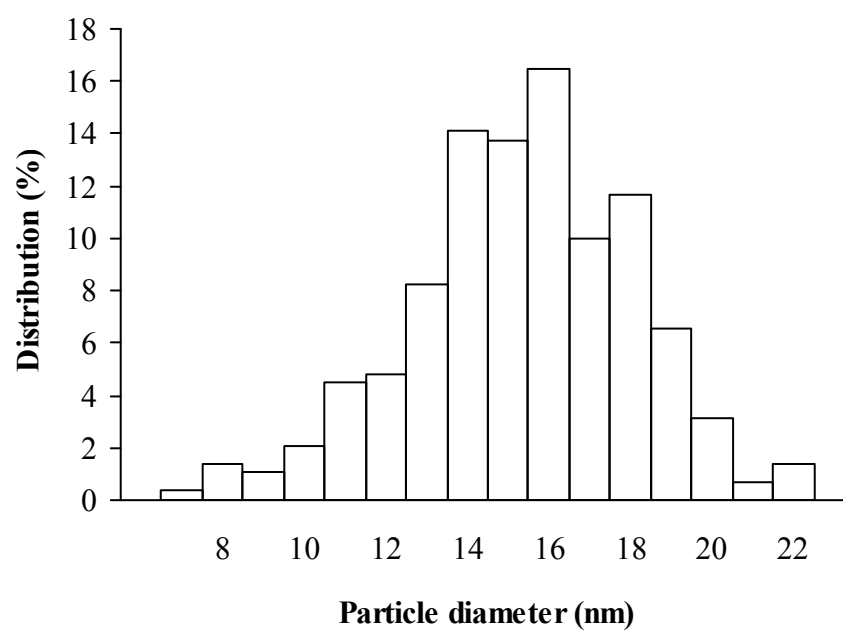


Figure 18 TEM images of PEI-stabilized AuNPs after preparation (A, B) and 1 month storage (C, D)

A



B

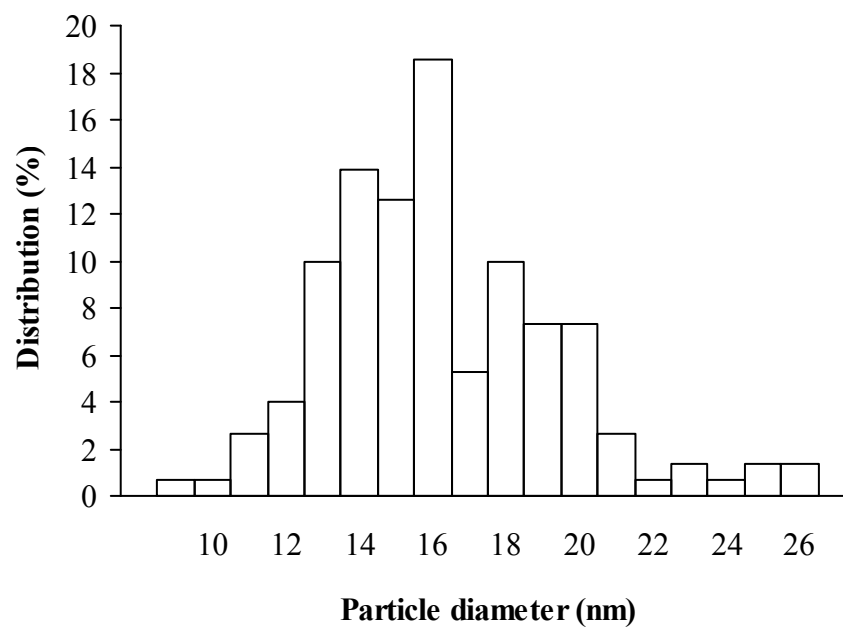
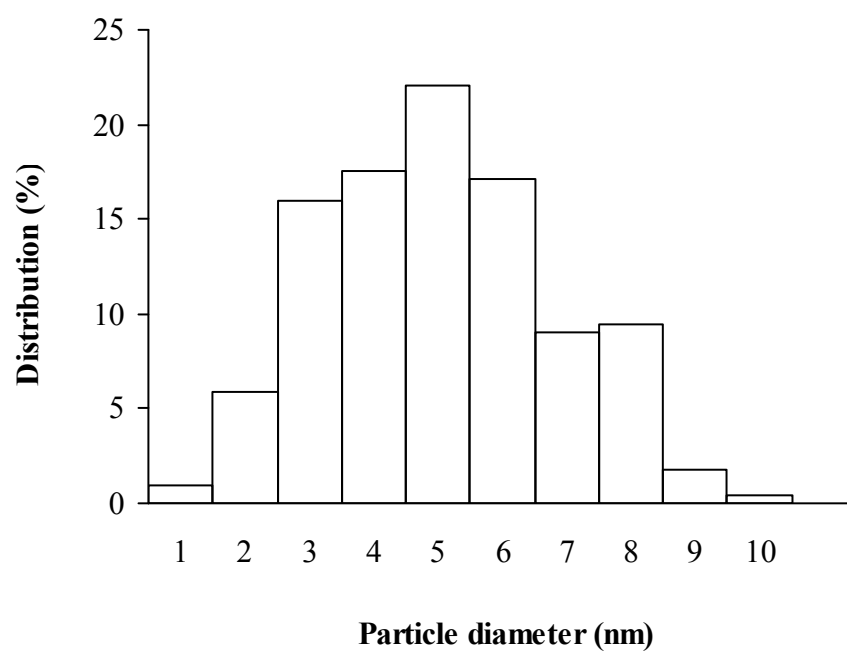


Figure 19 Size distributions of citrate-stabilized AuNPs after preparation (A) and 1 month storage (B)

A



B

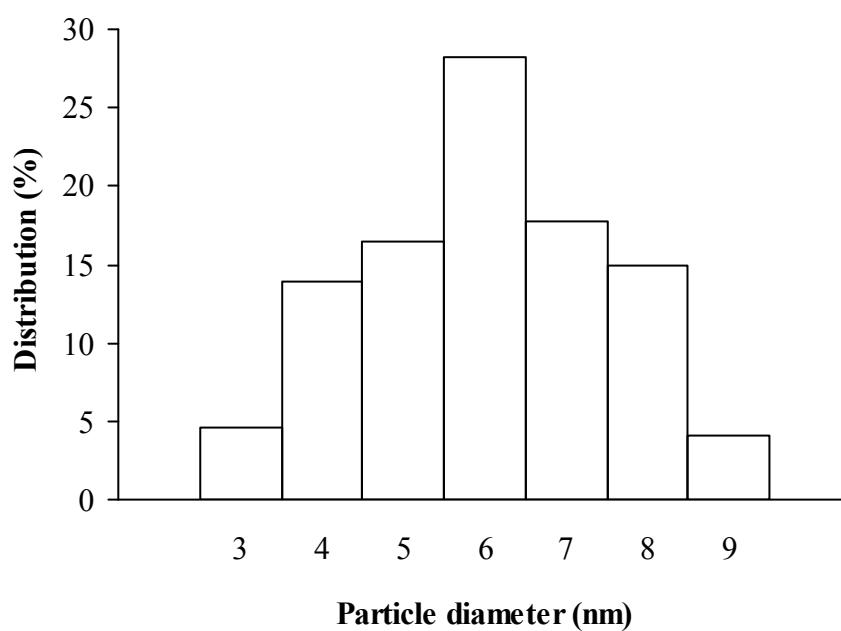


Figure 20 Size distributions of PEI-stabilized AuNPs after preparation (A) and 1 month storage (B)

2. Cytotoxicity test

MTT assay was used to determine cytotoxicity of AuNPs prepared using condition 1 on HepG2 cell line. AuCi at concentrations ranging from 0.1-90 μM (Au atom) showed very little toxicity (Figure 21). The results were in an agreement with a previous report which showed that citrate stabilized AuNPs at the concentration up to 250 μM were nontoxic to human leukemia cell line, K562 even though they were taken up into the cells (Conner *et al.*, 2005). On the other hand, AuPEI seemed to have more cytotoxicity on HepG2 cells with the IC_{50} of $37.58 \pm 1.15 \mu\text{M}$ (Figure 22). The higher cytotoxicity of AuPEI might be the result of the smaller size of AuPEI which was easier to enter through the cell membrane. A study reported that smaller particles presented the greater uptake and dispersed quickly to almost all tissues while larger particles were not (Aillon *et al.*, 2009; Foged *et al.*, 2005). Surface charge of the particles is another issue to be considered. Results from section 1.3 showed negative charge of $-40.60 \pm 1.22 \text{ mV}$ for AuCi and positive charge of $8.10 \pm 1.59 \text{ mV}$ for AuPEI. A previous report showed that LD_{50} of cationic AuNP (quaternary ammonium stabilized AuNP) was $\sim 1 \mu\text{M}$ while anionic (carboxylic acid stabilized AuNP) was more than $7.37 \mu\text{M}$ in kidney of the African green monkey (Cos-1) cell line suggesting that the anionic coating might not effectively interact with the overall negative charge of the lipid bilayer in cell membrane (Godman *et al.*, 2004). Recently, there was a study reported that positively charged nanoparticles had a greater interaction with human breast cancer cells than the negatively charged nanoparticles (Osaka *et al.*, 2009).

The non-toxic concentrations of AuNPs (more than 90% viability) were chosen as 1 and 10 μM for AuCi, and 0.1 and 1 μM for AuPEI in order to further investigate the effect of AuNPs on gene expression.

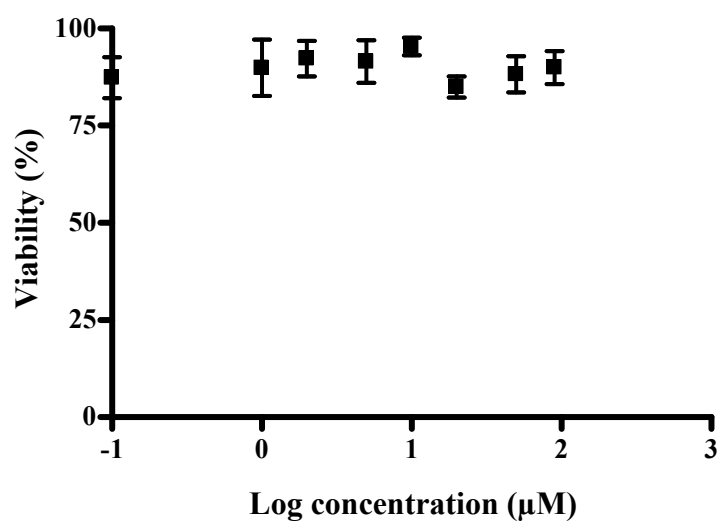


Figure 21 Cytotoxicity test of AuCi on HepG2 cells

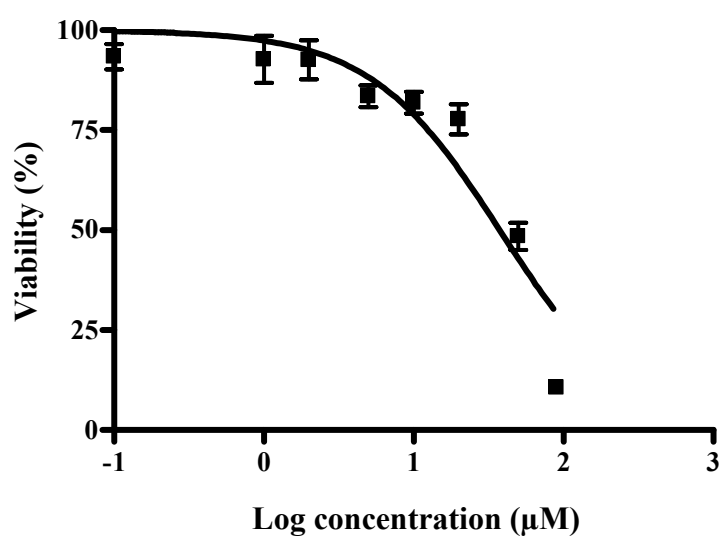

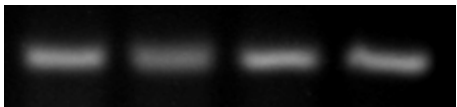
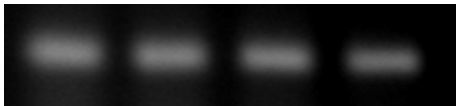
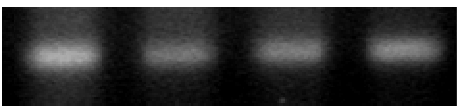
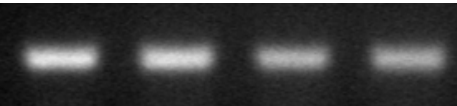
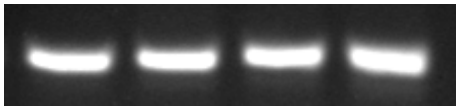


Figure 22 Cytotoxicity test of AuPEI on HepG2 cells

3. Verification of CYP gene in HepG2 cell line

Annealing is a step of PCR that the primers bind to the DNA templates. The higher temperature might be a barrier of the attachment, resulting in a fewer amplified DNA, but the lower temperature could allow more of the non-specific attachment. Hence, verifying for the suitable annealing temperature were performed with a gradient PCR machine and gel electrophoresis in the detection of CYP450 gene in HepG2 cell line. The experiment was set at four different annealing temperatures while denaturation and extension were made at 95°C and 72°C in orderly. The PCR products were run through agarose gels and taken images with GelDoc™ machine. The luminescence of the bands implied amount of PCR products detected (Table 3). From the results, it could be seen that all CYP genes were presented in HepG2 cell line. CYP2E1 and CYP3A4 were found at dominant levels while CYP1A1 was found at the lowest amount. The result was in agreement with Sumida *et al.* (2000) and Westerink and Schoonen (2007). The annealing temperatures in the range of 54-60°C did not show much difference in the amplified products. Thus, the annealing temperature of 60.0°C was chosen for further experiment since the higher temperature provides more specificity of annealing (Lewin, 2008).

Table 3 Gel electrophoresis of PCR products of CYP genes with different annealing temperatures

Gene	Product length (base pair)	Annealing temperature (°C)			
		60.0	58.8	56.2	54.0
CYP1A1	171				
CYP1A2	94				
CYP2C9	383				
CYP2E1	117				
CYP3A4	78				
GAPDH	151				

4. Investigation of gold nanoparticles influence on CYP mRNA expression

The effects of AuNPs on the expression of the CYP genes were investigated by real-time RT-PCR method and were analyzed using the $2^{-\Delta\Delta Ct}$ method which was used to calculate the relative quantification. The fold inductions of inducers and a mixture of inducers and AuNPs on CYP mRNA expressions are illustrated in Figures 23-32.

4.1 CYP1A1

From the results, an inducer, α NF significantly induced CYP1A1 mRNA expression to 3.30 ± 0.82 fold compared to the untreated cells. However, 18-fold induction of CYP1A1 after 9 h incubation was reported (Ishida *et al.*, 2002). The less fold induction found in the present study might be due to the different incubation time. AuCi at 1 μ M did not have significant effect on gene expression (1.17 ± 0.35 fold) while AuPEI at the same concentration induced CYP1A1 significantly at 1.68 ± 0.35 fold. Although the higher concentration of AuCi up to 10 μ M induced the gene at a higher fold (1.51 ± 0.38 fold), it still had no significant effect whereas the lower concentration of AuPEI at 0.1 μ M also induced the gene significantly to 1.66 ± 0.17 fold (Figure 23).

For the studies on an influence of AuNPs on inducer-induced gene expression showed that 1 μ M AuCi decreased the fold induction significantly from 3.30 ± 0.82 to 1.40 ± 0.34 while AuPEI decreased the inducing effect insignificantly to 2.29 ± 0.40 fold. The higher concentration of AuCi also showed significant influence on the inducer (fold induction = 1.58 ± 0.26). Surprisingly, the lower concentration of AuPEI at 0.1 μ M decreased the effect of inducer significantly (fold induction = 1.56 ± 0.54 , Figure 24).

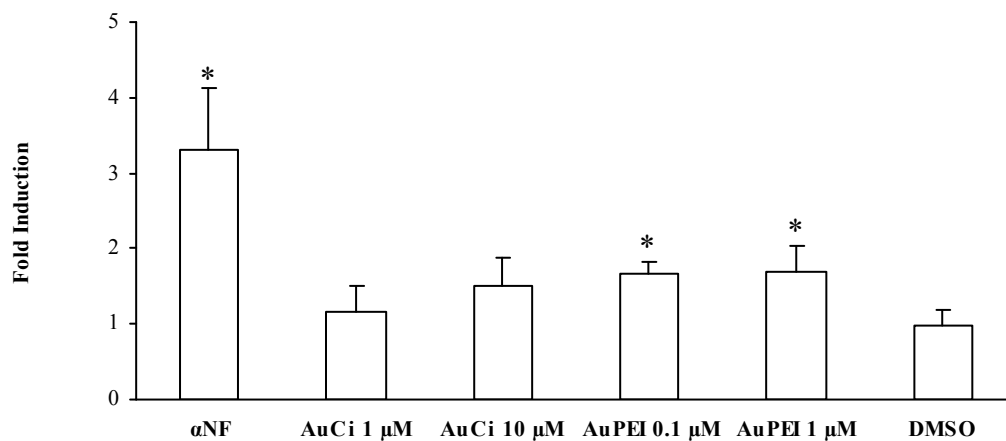


Figure 23 Fold induction of αNF (inducer), AuCi (1 and 10 μM), AuPEI (0.1 and 1 μM), and DMSO on CYP1A1 gene in HepG2 cells ($n=4$)

* Significantly different from an untreated control (= 1 fold), $p \leq 0.05$

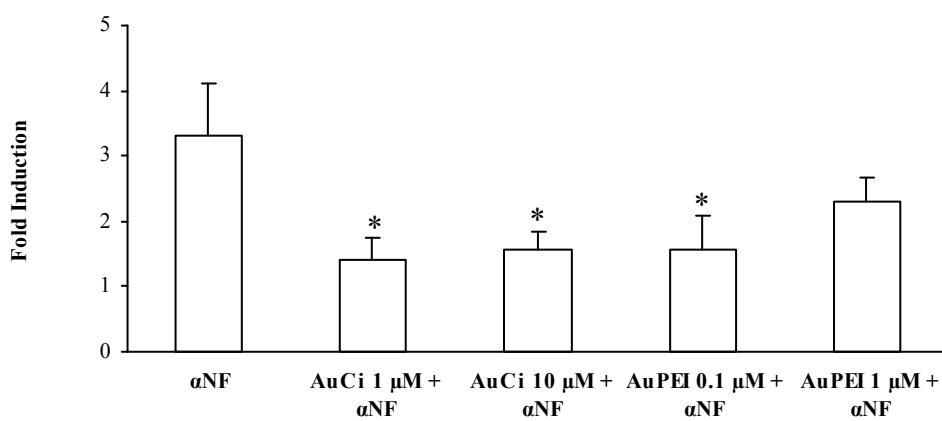


Figure 24 Fold induction of αNF (inducer), AuCi 1 μM + αNF, AuCi 10 μM + αNF, AuPEI 0.1 μM + αNF, and AuPEI 1 μM + αNF on CYP1A1 gene in HepG2 cells ($n=4$)

* Significantly different from an inducer, $p \leq 0.05$

4.2 CYP1A2

The inducer, α NF, could induce CYP1A2 up to 8.08 ± 2.41 fold which was similar to a previous report (Ishida *et al.*, 2002). From the results, AuCi at 1 μ M induced CYP1A2 insignificantly to 2.27 ± 0.83 fold while AuPEI at the same concentration induced the gene significantly at 2.08 ± 0.56 fold. However, an increase in the concentration of AuCi to 10 μ M caused a significant induction of the gene to 2.32 ± 0.35 fold while a decrease in concentration of AuPEI to 0.1 μ M caused an insignificantly induced the gene to 2.59 ± 1.00 fold (Figure 25).

The mixtures of AuCi and α NF showed a decrease in CYP1A2 induction from 8.08 ± 2.41 to 5.89 ± 0.49 and 2.69 ± 0.86 fold for 1 and 10 μ M, respectively. Interestingly, the mixture of the inducer and 1 μ M AuPEI increased the induction of the gene up to 12.70 ± 1.12 fold which was higher than inducer alone while the mixture of α NF and 0.1 μ M AuPEI insignificantly lowered the induction to 7.46 ± 0.96 fold (Figure 26).

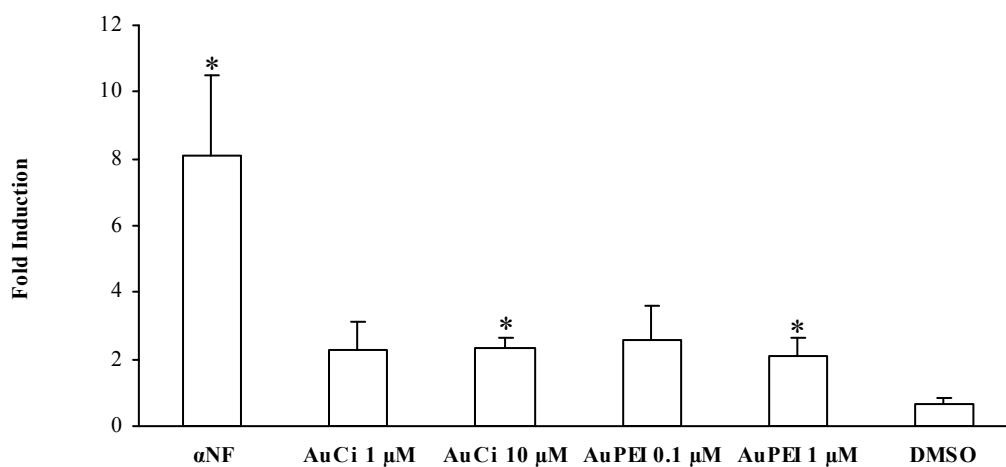


Figure 25 Fold induction of α NF (inducer), AuCi 1 μ M, AuCi 10 μ M, AuPEI 0.1 μ M, AuPEI 1 μ M, and DMSO on CYP1A2 gene in HepG2 cells ($n=4$)
 * Significantly different from an untreated control (= 1 fold), $p \leq 0.05$

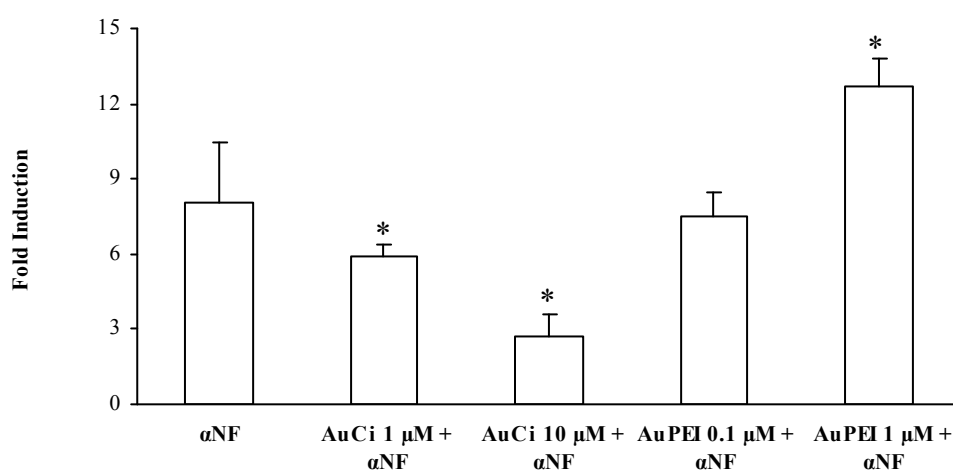


Figure 26 Fold induction of α NF (inducer), AuCi 1 μ M + α NF, AuCi 10 μ M + α NF, AuPEI 0.1 μ M + α NF, and AuPEI 1 μ M + α NF on CYP1A2 gene in HepG2 cells ($n=4$)
 * Significantly different from an inducer, $p \leq 0.05$

4.3 CYP2C9

Figure 27 shows that rifampicin significantly induced CYP2C9 gene for 3.00 ± 1.20 fold. One micromolar of AuNPs insignificantly induced CYP2C9 at 1.27 ± 0.40 and 1.11 ± 0.48 fold for AuCi and AuPEI, respectively. However, the higher concentration of AuCi (10 μ M) showed a significant induction of CYP2C9 gene up to 1.65 ± 0.39 fold.

A mixture of AuCi 1 μ M and rifampicin lowered the expression of CYP2C9 significantly to 0.76 ± 0.14 fold compared to induction by inducer alone. On the other hand, AuPEI at the same concentration insignificantly decreased the induction to 2.02 ± 0.29 fold. The higher concentration of AuCi (10 μ M) still decreased the induction significantly to 1.50 ± 0.41 fold while 0.1 μ M AuPEI caused a significant decrease in induction of the gene to 1.50 ± 0.52 fold (Figure 28).

4.4 CYP2E1

Ethanol significantly induced the gene to 1.42 ± 0.26 fold compared to the untreated control. The result was similar to a previous report that found an induction at 1.3 ± 0.1 fold (Alexandre *et al.*, 1999). AuPEI at 0.1 μ M also induced the gene significantly at 1.69 ± 0.27 fold while AuCi at 1 μ M, AuCi at 10 μ M, and AuPEI at 1 μ M insignificantly induced CYP2E1 at 1.12 ± 0.30 , 1.17 ± 0.45 , and 1.39 ± 0.88 folds, respectively (Figure 29). The mixtures of AuNPs (1 or 10 μ M AuCi and 0.1 or 1 μ M AuPEI) and ethanol decreased the induction insignificantly compared to ethanol inducer as seen in Figure 30.

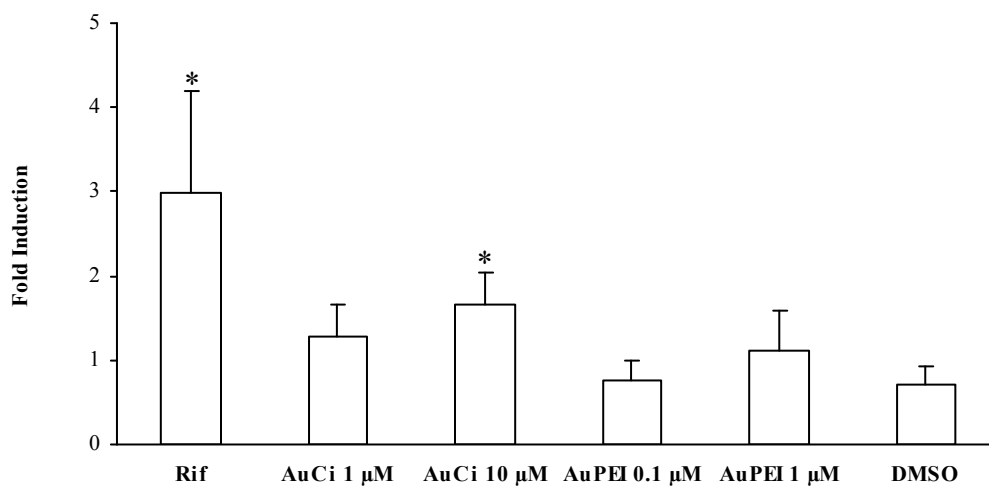


Figure 27 Fold induction of Rif (inducer), AuCi 1 μM, AuCi 10 μM, AuPEI 0.1 μM, AuPEI 1 μM, and DMSO on CYP2C9 gene in HepG2 cells ($n=4$)

* Significantly different from an untreated control (= 1 fold), $p \leq 0.05$

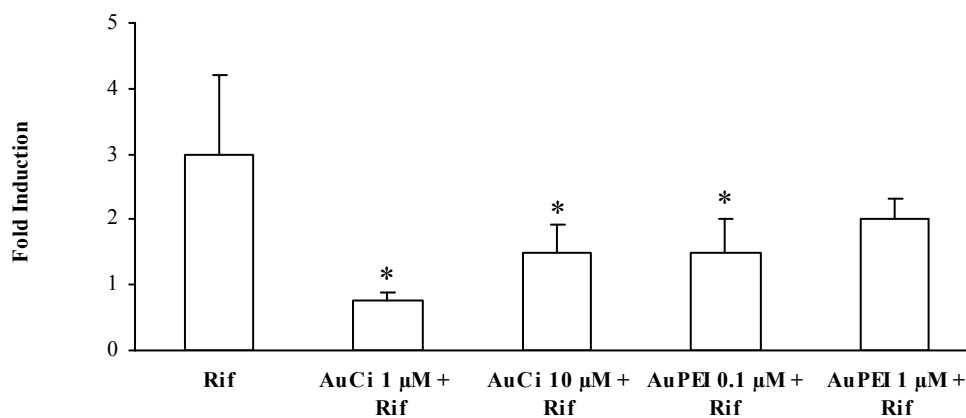


Figure 28 Fold induction of Rif (inducer), AuCi 1 μM + Rif, AuCi 10 μM + Rif, AuPEI 0.1 μM + Rif, and AuPEI 1 μM + Rif on CYP2C9 gene in HepG2 cells ($n=4$)

* Significantly different from an inducer, $p \leq 0.05$

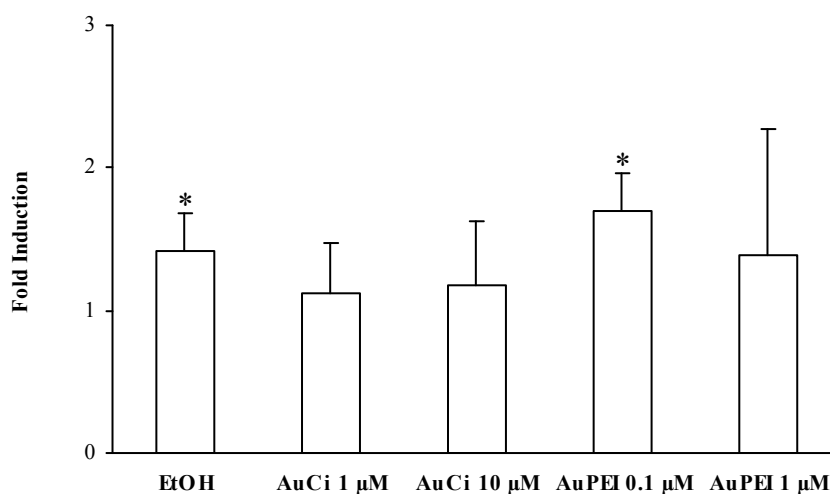


Figure 29 Fold induction of EtOH (inducer), AuCi 1 µM, AuCi 10 µM, AuPEI 0.1 µM, and AuPEI 1 µM on CYP2E1 gene in HepG2 cells ($n=4$)

* Significantly different from an untreated control (= 1 fold), $p \leq 0.05$

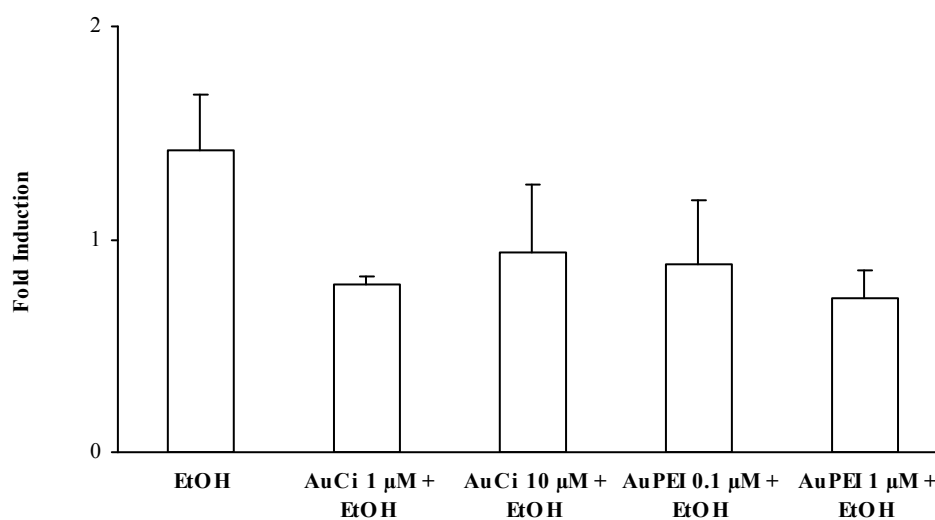


Figure 30 Fold induction of EtOH (inducer), AuCi 1 µM + EtOH, AuCi 10 µM + EtOH, AuPEI 0.1 µM + EtOH, and AuPEI 1 µM + EtOH on CYP2E1 gene in HepG2 cells ($n=4$)

* Significantly different from an inducer, $p \leq 0.05$

4.5 CYP3A4

AuNPs insignificantly induced CYP3A4 mRNA expression. Fold inductions of negatively charged AuCi were 1.03 ± 0.08 and 0.93 ± 0.30 for 1 and 10 μM , respectively while the positively charged AuPEI were 0.96 ± 0.15 and 0.64 ± 0.22 for 0.1 and 1 μM , in orderly (Figure 31). Rifampicin induced the gene at a significant level of 2.90 ± 0.91 fold which was similar to the work of Maruyama *et al.* (2007) and Westerink and Schoonen (2007).

In the presence of AuCi at 1 μM , significantly decreased CYP induction by rifampicin to 1.55 ± 0.10 fold was seen whereas AuPEI at the same concentration insignificantly decreased the induction of rifampicin. However, an increase in concentration of AuCi to 10 μM in the mixture of AuNPs and rifampicin caused an insignificant decrease while 0.1 μM AuPEI caused a significant decrease of induction to 1.61 ± 0.60 fold (Figure 32).

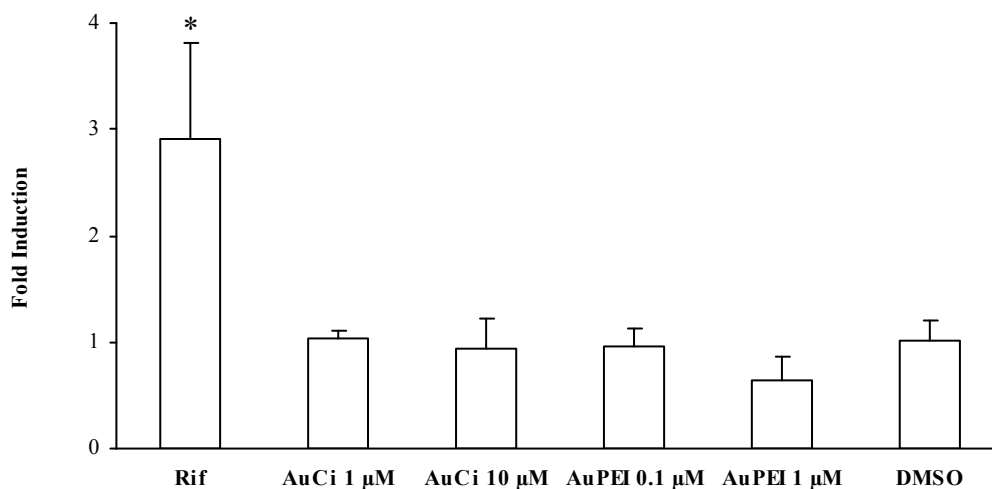


Figure 31 Fold induction of Rif (inducer), AuCi 1 μM, AuCi 10 μM, AuPEI 0.1 μM, AuPEI 1 μM, and DMSO on CYP3A4 gene in HepG2 cells ($n=4$)

* Significantly different from an untreated control (= 1 fold), $p \leq 0.05$

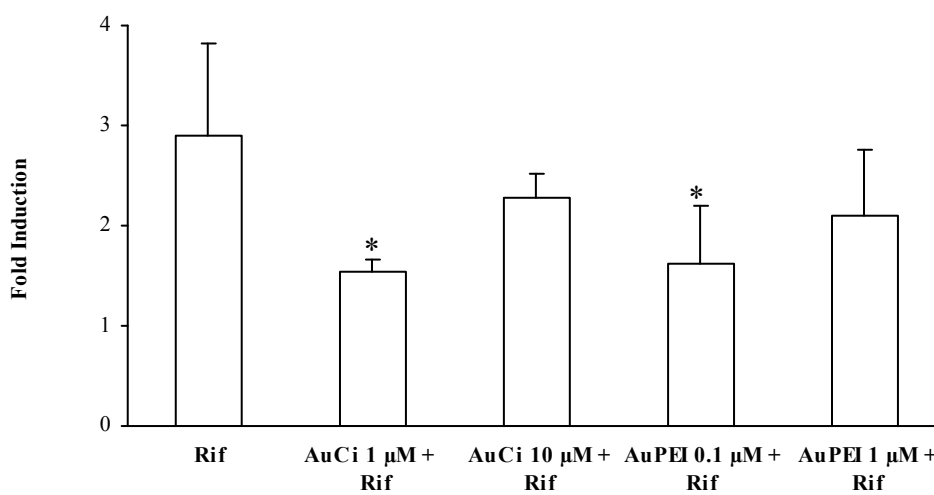


Figure 32 Fold induction of Rif (inducer), AuCi 1 μM + Rif, AuCi 10 μM + Rif, AuPEI 0.1 μM + Rif, and AuPEI 1 μM + Rif on CYP3A4 gene in HepG2 cells ($n=4$)

* Significantly different from an inducer, $p \leq 0.05$

In the present study, it was clearly seen that AuPEI mediated in CYP1A1 mRNA induction. On the other hand, AuCi did not show induction to the gene at the maximum concentration tested. The PEI is a positively charged molecule which enhances the particle to enter into the cell membrane which was covered by negative charges of the lipid bilayer (Goodman *et al.*, 2004). As far as resources available, none of metallic nanoparticles were tested with the CYP1A expression. However, some studies declared that the induction of CYP1A1 by heavy metals appeared to be cell-specific via multiple mechanisms (Elbekai and El-Kadi, 2005; Tully *et al.*, 2000). The metals induced mRNA by increasing the rate of transcription and, afterwards, decreasing the degradation of the mRNA transcripts (Elbekai and El-Kadi, 2007). The transcription of CYP1A1 is known by activating aryl hydrocarbon receptor (AHR) by its ligands. However, based on the structures of AHR's ligands and AHR-dependent mechanism, it is unlikely that the metals could bind to AHR directly (Denison and Nagy, 2003). Elbekai and El-Kadi (2007) suggested that AHR might be activated through an indirect mechanism. Metals may activate oxidative mechanisms and lead to develop creation of endogenous AHR ligands such as the release of arachidonic acid from glycerophospholipids in cells (Tournier *et al.*, 1997; Xu *et al.*, 2003).

Mechanisms of CYP1A2 induction by AuPEI may be applied with the CYP1A1 which was also activated through AHR. Krusekopf *et al.* (2003) proposed their work with the conclusion of xenobiotics that induced CYP1A1 mRNA expression were shown to induced CYP1A2 as well. Nevertheless, AuCi at higher concentrations showed significant induction of CYP1A2 mRNA. This might be

attributable to the longer half-life of CYP1A2 mRNA compared to CYP1A1 in HepG2 cells (Krusekopf *et al.*, 2003; Lekas *et al.*, 2000).

It can be seen that AuCi down regulated the effect of CYP1A1 and CYP1A2 transcription activated by α -NF. A similar study revealed that a combination of a metal, arsenite and an inducer, PAH, was less effective in an induction of CYP1A1 mRNA compared to the inducer alone (Vakharia *et al.*, 2001). Unpredictably, AuPEI 1 μ M had a synergist effect with an inducer and dramatically increased the CYP1A2 induction further. The result might relate to the positive charge of the particles which allow the particles to enter into the cells easier (Goodman *et al.*, 2004).

The basis of CYP2C9 induction was shown to be regulated by pregnane X receptor (PXR) and constitutive androstane receptor (CAR) (Al-Dosari *et al.*, 2005; Chen *et al.*, 2004). There is no evidence on CYP2C9 mRNA induction by gold nanoparticles. However, previous studies showed that CYP2C9 mRNA was downregulated by interleukin-6 which was elevated when incubated cultured human bronchial epithelial cell line (BEAS-2B) with titanium dioxide nanoparticles (Aitken and Morgan, 2007; Pascussi *et al.*, 2000; Park *et al.*, 2008).

AuPEI did not show any relation to CYP2C9 mRNA expression at the highest concentration tested. Interestingly, AuCi at 10 μ M showed a significant increase in the amount of gene expression probably via PXR/CAR. From the results, the mixtures of AuNPs with rifampicin were less effective than the inducer alone in the induction of CYP2C9 mRNA. Thus, AuNPs might interfere with the activation of rifampicin on PXR/CAR possibly due to the nano-sized of the particles induced an occurrence of inflammatory cytokines (Park *et al.*, 2008).

Since induction of CYP3A4 mRNA expression is activated via PXR (Gibson *et al.*, 2001; Quattrochi and Guzelian, 2001), the results implied that AuNPs at the maximum concentration tested had no interaction with the receptor. However, AuNPs lowered the ability of rifampicin in the induction of CYP3A4. In 2006, Inoue *et al.* showed that 14-nm nanoparticles significantly enhanced amounts of inflammatory cytokines, interleukin-2 and -10 which were found to decrease the CYP3A mRNA level (Tinel *et al.*, 1999). Chitosan nanoparticles were also found to increase nitric oxide which downregulated 50% of CYP3A4 mRNA (Pattani *et al.*, 2009; Aitken, Lee and Morgan, 2008).

Induction effect of CYP2E1 is known to be regulated in the post transcription level. Xenobiotics, ethanol and hormones may regulate the expression of CYP2E1 at a translational level (Kim *et al.*, 1990) and there were many studies showing that there was no positive correlation between the CYP2E1 mRNA and CYP2E1 protein (Abdelmegeed *et al.*, 2005; Kim *et al.*, 2001). The effect of ethanol on mRNA of CYP2E1 stabilization and/or translated activation was reported (Tsutsumi, Lasker, and Takahashi, 1993). Thus, this might explain the slight induction of CYP2E1 mRNA by ethanol and AuPEI at 0.1 μ M. Unexpectedly, a recent report by a group of Mohri *et al.* (2010) showed that expression of miR-378 (MRE378) in the 3'-untranslated region of human CYP2E1 mRNA was inversely correlated with the protein level of CYP2E1.

AuCi at higher concentration seemed to have more effect on CYPs and CYP1A2 was induced at the highest fold among tested CYPs as seen in Figure 33. Unlikely, AuPEI induced CYP1A1 at both concentration and CYP1A2 at higher

concentration. The lower concentration was insignificantly induced which might be due to the insufficient of data (Figure 34).

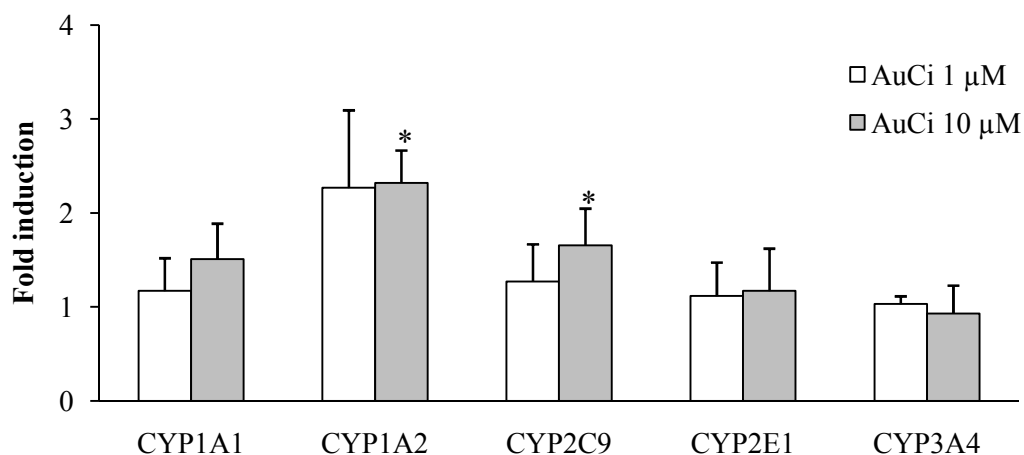


Figure 33 Fold induction of AuCi 1 μM and AuCi 10 μM on CYP1A1, CYP1A2, CYP2C9, CYP2E1 and CYP3A4 gene in HepG2 cells ($n=4$)

* Significantly different from an untreated control (= 1 fold), $p \leq 0.05$

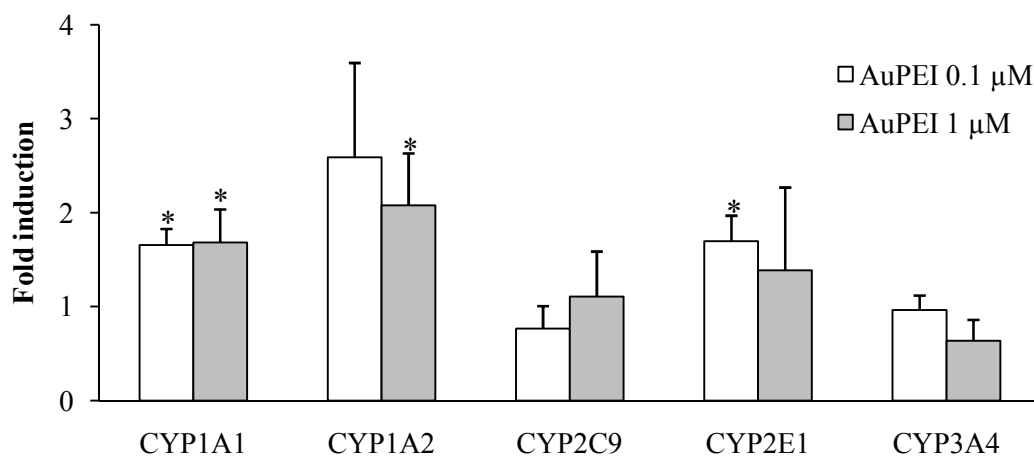


Figure 34 Fold induction of AuPEI 0.1 μM and AuPEI 1 μM on CYP1A1, CYP1A2, CYP2C9, CYP2E1 and CYP3A4 gene in HepG2 cells ($n=4$)

* Significantly different from an untreated control (= 1 fold), $p \leq 0.05$

When comparing each CYPs within the same treatment, AuCi 1 μ M seemed to have no relation with the treatment while AuPEI at the same concentration, on the other hand, caused a positive relation on CYP1A1 and CYP1A2 mRNA expression (Figure 35).

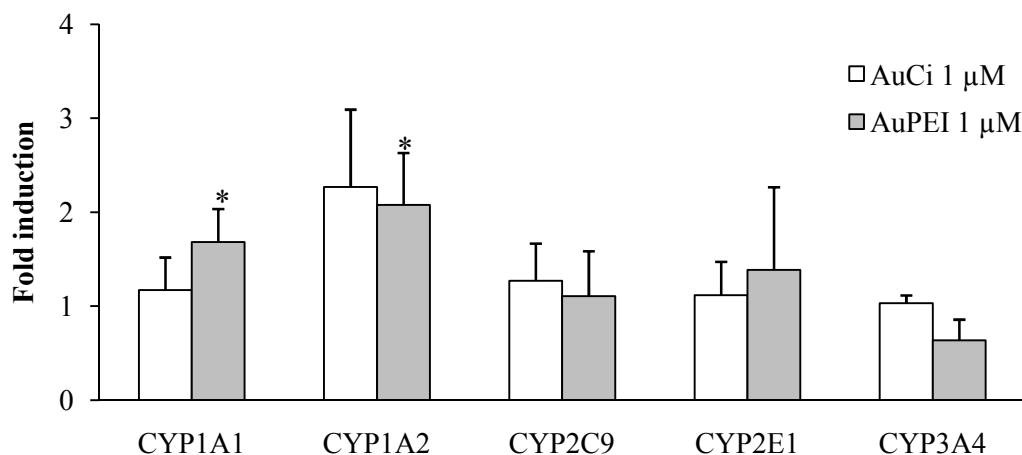


Figure 35 Fold induction of AuCi 1 μ M and AuPEI 1 μ M on CYP1A1, CYP1A2, CYP2C9, CYP2E1 and CYP3A4 gene in HepG2 cells ($n=4$)

* Significantly different from an untreated control (= 1 fold), $p \leq 0.05$

The mixture of inducers and the lower concentration of AuCi had stronger effects in the lowering induction of the inducers than the higher concentration on CYP3A4 and on CYP1A1, CYP2C9 and CYP3A4 for AuPEI. The results seemed to imply that the lower concentration of AuNPs might act as the more potent antagonist to the receptor than the higher concentration. An example for this might relate to some studies which showed that low concentrations of various flavanoids can act as AHR antagonist towards a strong agonist by competing for the binding to the receptor (Ashida *et al.*, 2000). In contrast, flavanoids at high concentrations may act as AHR agonists including transactivation of CYP1A1 genes (Lu *et al.*, 1996).

As discussed above, AuNPs could significantly induce three kinds of CYPs 1A1, 1A2, and 2C9. AuCi at 10 μ M induced CYP1A2 and CYP2C9 while AuPEI at 10 times lower concentration, 1 μ M, induced CYP1A1 and CYP1A2. It could be seen that higher concentration of AuCi than those of AuPEI was needed to induce the CYPs. It was possibly due to the fact that AuPEI contained positive charge which provides the easier entering of the particles into the cell membrane (Goodman *et al.*, 2004). AuNPs were also found to lower the effect of inducers. The mixtures of AuNPs and α NF or rifampicin were less effective in the induction of CYP1A1, CYP1A2, CYP2C9 and CYP3A4. The lowered effects were believed to perform indirectly, mostly via inflammatory chemicals in the cell triggered by the nano-sized particles.

For pharmaceutical, it can be stated that drug that produces an a change in activity of greater than 40% of the positive control (inducer) is considered as an enzyme inducer (U.S. Food and Drug Administration, 2006). If the chemical correlated with mRNA expression and activity of the enzyme, this criterion classified AuCi at 10 μ M as CYP1A1 and CYP2C9 inducer (45.76% and 55.00%, respectively) and AuPEI at 1 μ M as CYP1A1 inducer (50.90%). The results provide information on the use of AuNPs as nanomedicine. The lack of CYP induction offers a normal drug metabolism. If AuNPs can induce CYP, drugs that are metabolized by the CYP should be less effective. According to the results, AuNPs can be developed for delivery of drug metabolized by CYP3A4 which are responsible for the metabolism of the most drugs metabolized by CYPs. This study showed that CYP induction potency seemed to depend on size and charge of AuNPs in that the smaller and positively

charged can more effective in CYP induction. However, the mechanism of how AuNPs affect the CYP induction should be further clarified.

CHAPTER V

CONCLUSION

The novel pharmaceutical material has put more interests on AuNPs according to their variety of applications. The special characteristics of AuNPs include the tiny sizes, high surface area, biocompatibility, and optical properties which can be applied to various uses of AuNPs such as biosensors, drug delivery and imaging. Due to the assorted application of AuNPs, cytotoxicity and effect of them on CYP inductions were investigated. AuNPs were synthesized using citrate and PEI as stabilizers and investigated for their effects on CYP1A1, CYP1A2, CYP2C9, CYP2E1, and CYP3A4 mRNA inductions using real-time PCR method.

AuNPs were synthesized using various molar ratios of Au to stabilizers, citrate (for AuCi) and PEI (for AuPEI). The suitable ratio for AuCi was found at 4:1 while AuPEI was found at 0.35:1. Average sizes of citrate and PEI-stabilized AuNPs were 15.00 ± 2.77 and 5.02 ± 1.81 nm, respectively. Slight increase in sizes was observed after a month of storage time. Citrate-stabilized AuNP seemed to have no cytotoxicity on HepG2 cell line at a maximum concentration used ($90 \mu\text{M}$). In contrast, cytotoxicity of PEI-stabilized AuNP was found with the IC_{50} value of $37.58 \pm 1.15 \mu\text{M}$.

Three CYPs, CYP1A1, CYP1A2, and CYP2C9, were found to be significantly induced by AuNPs. AuCi at a concentration of $10 \mu\text{M}$ induced CYP1A2 and CYP2C9 while AuPEI at a concentration of $1 \mu\text{M}$ induced CYP1A1 and CYP1A2. The inductions of CYP1A1 and CYP1A2 mRNA might be activated

indirectly through activation of arachidonic acid in cells leading to the higher amount of AHR ligand which is responsible for CYP1A induction (Tournier *et al.*, 1997; Xu *et al.*, 2003). None of significant inductions by AuNPs were found for CYP3A4. However, weak induction of CYP2E1 mRNA by AuNPs was observed since it was regulated in the post-transcriptional step. It seemed that AuPEI had the higher effect on CYP induction at the lower concentration than that of AuCi which might be due to the smaller size (3 times smaller than AuCi) and the positive charges of AuPEI (8.10 ± 1.59 mV) which could support the cellular penetration.

AuNPs were also found to lower the effect of specific inducers of CYPs. The mixtures of AuCi (1 μ M) and CYP inducers (α -naphthoflavone (α NF) for CYP1A or rifampicin for CYP2C9 and CYP3A4) were significantly less effective in the inductions of CYP1A1, CYP1A2, CYP2C9 and CYP3A4 compared to the corresponding inducers alone. Similarly, the mixtures of AuPEI (0.1 μ M) and CYP inducers had less induction of CYP1A1, CYP2C9 and CYP3A4 at a significance level ($p \leq 0.05$) compared to the corresponding inducers. Notably, the mixture of AuPEI (1 μ M) and α NF was found to induce CYP1A2 greater than α NF alone which might be due to the nanosized (~ 5 nm) and positive charges of the particles. The down-regulation of inducer-induced CYPs in the presence of AuNPs was believed to perform indirectly, mostly *via* inflammatory chemicals excreted from the cells by triggering of the nano size of the particles. From the overall results, AuNPs might interfere in metabolism of drug metabolized by CYP. The suggestion for further study would be the clarification on the mechanism of CYP induction by AuNPs.

REFERENCES

- Aaseth, J.; Haugen, M.; and Forre, O. 1998. Rheumatoid arthritis and metal compounds-perspectives on the role of oxygen radical detoxification. Analyst 123: 3-6.
- Abdelmegeed, M. A.; Carruthers, N. J.; Woodcroft, K. J.; Kim, S. K.; and Novak, R. F. 2005. Acetoacetate induced CYP2E1 protein and suppresses CYP2E1 mRNA in primary cultured rat hepatocytes. J. Pharmacol. Exp. 315: 203-213.
- Aillon, K. L.; Xie, Y.; El-Gendy, N.; Berkland, C. J.; and Forrest, M. L. 2009. Effects of nanomaterial physicochemical properties on *in vivo* toxicity. Adv. Drug Deliv. Rev. 61: 457-466.
- Aitken A. E.; and Morgan, E. T. 2007. Gene-specific effects of inflammatory cytokines on cytochrome P450C, 2B6 and 3A4 mRNA levels in human hepatocytes. Drug Metab. Dispos. 35: 1687-1693.
- Aitken, A. E.; Lee, C.; and Morgan, E. T. 2008. Roles of nitric oxide in inflammatory downregulation of human cytochromes P450. Free Radic. Biol. Med. 44: 1161-1168.
- Al-Dosari, M. S.; Knapp, J. E.; Liu, D. 2005. Activation of human CYP2C9 promoter and regulation by CAR and PXR in mouse liver. Mol. Pharm. 3: 322-328.
- Alexandre, E.; David, P.; Viollon, C.; Wolf, P.; Jaeck, D.; Azimzadeh, A.; Nicod, L.; Boudjema, K.; and Richert, L. 1999. Expression of cytochrome P-450 2E1, 3A4 and 1A1/1A2 in growing and confluent human HepG2 hepatoma cells-effect of ethanol. Toxicol. In Vitro 13: 427-435.

- Alivisatos, P. 2004. The use of nanocrystals in biological detection. Nat. Biotechnol. 22: 47-52.
- Ashida, H.; Fukuda, I.; Yamashita, T.; and Kanazawa, K. 2000. Flavones and flavonols at dietary levels inhibit a transformation of aryl hydrocarbon receptor induced by dioxin. FEBS Lett. 476: 213-217.
- Baptista, P.; Pereira, E.; Eaton, P.; Doria, G.; Miranda, A.; Gomes, E.; Quaresma, P.; and Franco, R. 2007. Gold nanoparticles for the development of clinical diagnosis methods. Anal. Bioanal. Chem. 391: 943-950.
- Bhattacharya, R.; Patra, C. R.; Verma, R.; Kumar, S.; Greipp, P. R.; and Mukherjee, P. 2007. Gold nanoparticles inhibit the proliferation of multiple myeloma cells. Adv. Mater. Weinheim 19: 711-716.
- Bhattacharya, R.; and Mukherjee, P. 2008. Biological properties of “naked” metal nanoparticles Adv. Drug Deliv. Rev. 60: 1289-1306.
- Bibi, Z. 2008. Role of cytochrome P450 in drug interactions. Nutr. Metab. 5: 27.
- Burda, C.; Chen, X.; Narayanan, R.; and El-Sayed, M. A. 2005. Chemistry and properties of nanocrystals of different shapes. Chem. Rev. 105: 1025-1102.
- Chen, Y.; Ferguson, S. S.; Negishi, M.; and Goldstein, J. A. 2004. Induction of human *CYP2C9* by rifampicin, hyperforin, and Phenobarbital is mediated by the pregnane X receptor. J. Pharmacol. Exp. Ther. 308: 495-501.
- Chiu, S. L. 1993. The use of in vitro metabolism studies in the understanding of new drugs. J. Pharmacol. Toxicol. Methods 29: 77-83.
- Coleman, M. D. 2005. Human Drug Metabolism: An Introduction. Chichester: John Wiley and Sons.

- Conner, E. E.; Mwamuka, J.; Gole, A.; Murphy, C. J.; and Wyatt, M. D. 2005. Gold nanoparticles are taken up by human cells but do not cause acute cytotoxicity. Small 1: 325-327.
- Daniel, M. C.; and Astruc, D. 2004. Gold nanoparticles: assembly, supramolecular chemistry, quantum-size-related properties, and applications toward biology, catalysis, and nanotechnology. Chem. Rev. 104: 293-346.
- Denison, M. S.; and Nagy, S. R. 2003. Activation of the aryl hydrocarbon receptor by structurally diverse exogenous and endogenous chemicals. Annu. Rev. Pharmacol. Toxicol. 43: 309-334.
- Dorrenhaus, A.; Muller, T.; and Roos, P. H. 2007. Increased CYP1A1 expression in human exfoliated urothelial cells of cigarette smokers compared to non-smokers. Arch. Toxicol. 81: 19-25.
- Elbekai, R. H.; and El-Kadi, A. O. 2005. The role of oxidative stress in the modulation of aryl hydrocarbon receptor-regulated genes by As^{3+} , Cd^{2+} , and Cr^{6+} . Free Radic. Biol. Med. 39: 1355-1367.
- Elbekai, R. H.; and El-Kadi, A. O. 2007. Transcriptional activation and posttranscriptional modification of CYP1A1 by arsenite, cadmium, and chromium. Toxicol. Lett. 172: 106-119.
- El-Sayed, M. A. 2001. Some interesting properties of metals confined in time and nanometer space of different shapes. Acc. Chem. Res. 34: 257-264.
- El-Sayed, I. H.; Huang, X.; and El-Sayed, M. A. 2005. Surface Plasmon resonance scattering and absorption of anti-EGFR antibody conjugated gold nanoparticles in cancer diagnostics: applications in oral cancer. Nano Lett. 5: 829-834.

- El-Sayed, I. H.; Huang, X.; and El-Sayed, M. A. 2006. Selective laser photo-thermal therapy of epithelial carcinoma using anti-EGFR antibody conjugated gold nanoparticles. Cancer Lett. 239: 129-135.
- Foged, C.; Brodin, B.; Frokjaer, S.; and Sundblad, A. 2005. Particle size and surface charge affect particle uptake by human dendritic cells in an *in vivo* model. Int. J. Pharm. 298: 315-322.
- Gannon, C. J.; Patra, C. R.; Bhattacharya, R.; Mukherjee, P.; and Curley, S. A. 2008. Intracellular gold nanoparticles enhance non-invasive radiofrequency thermal destruction of human gastrointestinal cancer cells. J. Nanobiotechnol. 6:2.
- Gibson, G. G.; Plant, N. J.; Swales, K. E.; Ayrton, A.; and El-Sankary, W. 2001. Receptor-dependent transcriptional activation of cytochrome P4503A genes: Induction mechanisms, species differences and interindividual variation in man. Xenobiotica 32: 165-206.
- Gibson, J. D.; Khanal, B. P.; and Zubarev, E. R. 2007. Paclitaxel-functionalized gold nanoparticles. J. Am. Chem. Soc. 129: 11653-11661.
- Gibson, N.; Shenderova, O.; Luo, T. J. M.; Moseenkov, S.; Bondar, V.; Puzyr, A.; Purto, K.; Fitzgerald, Z.; and Brenner, D. W. 2009. Colloid stability of modified nanodiamond particles. Diam. and Relat. Mater. 18: 620-626.
- Goodman, C. M.; McCusker, C. D.; Yilmaz, T.; and Rotello, V. M. 2004. Toxicity of gold nanoparticles functionalized with cationic and anionic side chains. Bioconjug. Chem. 15: 897-900.
- Goshman, L.; Fish, J.; and Roller, K. 1999. Clinically significant cytochrome P450 drug interactions. J. Pharm. Soc. Wis. May/June: 23-38.

- Guengerich, F. P. 2004. Cytochrome P450: what have we learned and what are the future issues? Drug Metab. Rev. 35: 159-197.
- Haiss, W.; Thank, N. T. K.; Aveyard, J.; and Fernig, D. G. 2007. Determination of size and concentration of gold nanoparticles from UV-Vis spectra. Anal. Chem. 79: 4215-4221.
- Hauck, T. S.; Ghazani, A. A.; and Chan, W. C. W. 2008. Assessing the effect of surface chemistry on gold nanorod uptake, toxicity, and gene expression in mammalian cells. Small 4: 153-159.
- Hubbard, A. T. 2002. Encyclopedia of Surface and Colloid Science. New York: Marcel Dekker.
- Hukkanen, J. 2000. Xenobiotic-metabolizing cytochrome P450 enzymes in human lung. Acta Univ Oul. D621.
- Inoue, K.; Takano, H.; Yanagisa, R.; Ichinose, T.; Sakurai, M.; and Yoshikawa, T. 2006. Effects of nano particles on cytokine expression in murine lung in the absence or presence of allergen. Arch. Toxicol. 80: 614-619.
- Ishida, S.; Jinno, H.; Tanaka-Kagawa, T.; Ando, M.; Ohno, Y.; Ozawa, S.; and Sawada, J. 2002. Characterization of human *CYP1A1/1A2* induction by DNA microarray and α -naphthoflavone. Biochem. Biophys. Res. Commun. 296: 172-177.
- Kawajiri, K.; and Fujii-Kuriyama, Y. 2007. Cytochrome P450 gene regulation and physiological functions mediated by the aryl hydrocarbon receptor. Arch. Biochem. Biophys. 464: 207-212.
- Khan, J. A.; Pillai, B.; Das, T. K.; Singh, Y.; and Maiti, S. 2007. Molecular effects of uptake of gold nanoparticles in HeLa cells. Chembiochem. 8: 1237-1240.

- Khlebtsov, N. G. 2008. Determination of size and concentration of gold nanoparticles from extinction spectra. Anal. Chem. 80: 6620-6625.
- Kim, S. G.; Shehin, S. E.; States, C.; and Novak, R. F. 1990. Evidence for increased translational efficiency in the induction of P450IIE1 by solvents: Analysis of P450IIE1 mRNA polyribosomal distribution. Biochem. Biophys. Res. Commun. 172: 767-774.
- Kim, H.; Putt, D. A.; Zangar, R. C.; Wolf, C. R.; Guengerich, F. P.; Edwards, R. J.; Hollenberg, P. F.; and Novak, R. F. 2001. Differential induction of rat hepatic cytochromes P450 3A1, 3A2, 2B1, 2B2, and 2E1 in response to pyridine treatment. Drug Metab. Dispos. 29: 353-360.
- Kimling, J.; Maier, M.; Okenve, B.; Kotaidis, V.; Ballot, H.; and Plech, A. 2006. Turkevich method for gold nanoparticles synthesis revisited. J. Phys. Chem. B 110: 15700-15707.
- Kiss, I.; Orsos, Z.; Gombos, K.; Bogner, B.; Csejtei, A.; Tibold, A.; Varga, Z.; Pazsit, E.; Magda, I.; Zolyomi, A.; and Ember, I. 2007. Association between allelic polymorphisms of metabolizing enzymes (CYP1A1, CYP1A2, CYP2E1, mEH) and occurrence of colorectal cancer in Hungary. Anticancer Res. 27: 2931-2937.
- Köth, A.; Koetz, J.; and Appelhans, D. 2008. Sweet gold nanoparticles with oligosaccharide-modified poly(ethyleneimine). Colloid Polym. Sci. 286: 1317-1327.
- Kronberg, B.; Dahlman, A.; Carlfors, J.; Karlsson, J.; and Artursson, P. 1990. Preparation and evaluation of sterically stabilized liposomes: colloidal

- stability, serum stability, macrophage uptake, and toxicity. J. Pham. Sci. 79: 667-671.
- Krusekopf, S.; Roots, I.; Hilderbrandt, A. G.; and Kleeberg, U. 2003. Time-dependent transcriptional induction of CYP1A1, CYP1A2 and CYP1B1 mRNAs by H⁺/K⁺-ATPase inhibitors and other xenobiotics. Xenobiotica 33: 107-118.
- Kumar, S.; Gandhi, K. S.; and Kumar, R. 2007. Modeling of formation of gold nanoparticles by citrate method. Ind. Eng. Chem. Res. 46: 3128-3136.
- Lekas, P.; Tin, K. L.; Lee, C.; and Prokipcak, R. D. 2000. The human cytochrome P450 1A1 mRNA is rapidly degraded in HepG2 cells. Arch. Biochem. Biophys. 384: 311-318.
- Levitz, S. M.; and Diamond, R. D. 1985. A rapid colorimetric assay of fungal viability with the tetrazolium salt MTT. J. Infect. Dis. 152: 938-945
- Lewin, B. 2008. Genes IX. London: Jones and Bartlett.
- Livak, K. J.; and Schmittgen, T. D. 2001. Analysis of relative gene expression data using real-time quantitative PCR and the 2^{- $\Delta\Delta C_t$} method. Methods 25: 402-408.
- Lu, Y. F.; Santostefano, M.; Cunningham, B. D. M.; Threadgill, M. D.; and Safe, S. 1996. Substituted flavones as aryl hydrocarbon (Ah) receptor agonists and antagonists. Biochem Pharmacol. 51: 1077-1087.
- Maruyama, M.; Matsunaga, T.; Harada, E.; and Ohmori, S. 2007. Comparison of basal gene expression and induction of CYP3As in HepG2 and human fetal liver cells. Biol. Pharm. Bull. 30: 2091-2097.

- Mohri, T.; Nakajima, M.; Fukami, T.; Takamiya, M.; Aoki, Y.; and Yokoi, T. 2010. Human CYP2E1 is regulated by miR-378. Biochem. Pharmacol. 79: 1045-1052.
- Mukherjee, P.; Bhattacharya, R.; Wang, P.; Wang, L.; Basu, S.; Nagy, J. A.; Atala, A.; Mukhopadhyay, D.; and Soker, S. 2005. Antiangiogenic properties of gold nanoparticles. Clin. Cancer. Res. 11: 3530-3534.
- Mukherjee, P.; Bhattacharya, R.; Bone, N.; Lee, YK.; Patra, C. R.; Wang, S.; Lu, L.; Secreto, C.; Banerjee, P. C.; Yaszemski, M. J.; Kay, N. E.; and Mukhopadhyay, D. 2007. Potential therapeutic application of gold nanoparticles in B-chronic lymphocytic leukemia (BCLL): enhancing apoptosis. J. Nanobiotechnol. 5: 4.
- Murphy, C. J.; Gole, A. M.; Stone, J. W.; Sisco, P. N.; Alkilany, A. M.; Goldsmith, E. C.; and Baxter, S. C. 2008. Gold nanoparticles in biology: beyond toxicity to cellular imaging. Acc. Chem. Res. 41: 1721-1730.
- Nelson, D. R.; Zeldin, D. C.; Hoffman, S. M.; Maltais, L. J.; Wain, H. M.; and Nebert, D. W. 2004. Comparison of cytochrome P450 (CYP) genes from the mouse and human genomes, including nomenclature recommendations for genes, pseudogenes and alternative-splice variants. Pharmacogenetics 14: 1-18.
- Note, C., Kosmella, S. and Koetz, J. 2006. Poly(ethyleneimine) as reducing and stabilizing agent for the formation of gold nanoparticles in w/o microemulsions. Colloid Surf. A. 290: 150-156.
- Osaka, T.; Nakanishi, T.; Shanmugam, S.; Takahama, S.; and Zhang, H. 2009. Effect of surface charge of magnetite nanoparticles on their internalization into breast

- cancer and umbilical vein endothelial cells. Colloids Surf. B Biointerfaces 71: 325-330.
- Papis, E.; Gornati, R.; Prati, M.; Ponti, J.; Sabbioni, E.; and Bernardini, G. 2007. Gene expression in nanotoxicology research: analysis by differential display in BALB3T3 fibroblasts exposed to cobalt particles and ions. Toxicol. Lett. 170: 185-192.
- Park, E.; Yi, J.; Chung, K.; Ryu, D.; Choi, J.; and Park, K. 2008. Oxidative stress and apoptosis induced by titanium dioxide nanoparticles in cultured BEAS-2B cells. Toxicol. Lett. 180: 222-229.
- Pascussi, J. M.; Gerbal-Chaloin, S.; Pichard-Garcia, L.; Daujat, M.; Fabre, J. M.; Maurel, P.; and Vilarem, M. J. 2000. Interleukin-6 negatively regulates the expression of pregnane x receptor and constitutively activated receptor in primary human hepatocytes. Biochem. Biophys. Res. Commun. 274: 707-713.
- Patra, C. R.; Bhattacharya, R.; Wang, E.; Katarya, A.; Lau, J. S.; Dutta, S.; Muders, M.; Wang, S.; Buhrow, S. A.; Safgren, S. L.; Yaszemski, M. J.; Reid, J. M.; Ames, M. M.; Mukherjee, P.; and Mukhopakhyay, D. 2008. Targeted delivery of gemcitabine to pancreatic adenocarcinoma using cetuximab as a targeting agent. Cancer Res. 68: 1970-1978.
- Pattani, A.; Patravale, V. B.; Panicker, L.; and Potdar, P. D. 2009. Immunological effects and membrane interactions of chitosan nanoparticles. Mol. Pharm. 6: 345-352.
- Pong, B. K.; Elim, H. I.; Chong, J. X.; Ji, W.; Trout, B. L.; and Lee, J. Y. 2007. New insights on the nanoparticles growth mechanism in the citrate reduction of

- gold (III) salt: Formation of the Au nanowire intermediate and its nonlinear optical properties. J. Phys. Chem. 111: 6281-6287.
- Quattrochi, L. C.; and Guzelian, P. S. 2001. CYP3A regulation: From pharmacology to nuclear receptors. Drug Metab. Dispos. 29: 615-622.
- Roberts-Thomson, S. J.; McManus, M. E.; Tukey, R. H.; Gonzalez, F. F.; and Holder, G. M. 1993. The catalytic activity of four expressed human cytochrome P450s towards benzo[a]pyrene and the isomers of its proximate carcinogen. Biochem. Biophys. Res. Commun. 192: 1373-1379.
- Rosi, N. L.; Giljohann, D. A.; Thaxton, C. S.; Lytton-Jean, A. K. R.; Han, M. S.; and Mirkin, C. A. 2006. Oligonucleotide-modified gold nanoparticles for intracellular gene regulation. Science 312: 1027-1030.
- Schwarz, U. I. 2003. Clinical relevance of genetic polymorphisms in the human CYP2C9 gene. Eur. J. Clin. Invest. 33: 23-30.
- Shaik, S.; Cohen, S.; Wang, Y.; Chen, H.; Kumar, D.; and Thiel, W. 2010. P450 enzymes: their structure, reactivity, and selectivity – modeled by QM/MM calculations. Chem. Rev. 110: 949-1017.
- Shukla, R.; Vansal, V.; Chaudhary, M.; Basu, A.; Bhonde, R. R.; and Sastry, M. 2005. Biocompatibility of gold nanoparticles and their endocytotic fate inside the cellular compartment: a microscopic overview. Langmuir 21: 10644-10654.
- Sjöblom, J., 2006. Emulsions and emulsion stability. Taylor and Francis, New York.
- Sokolov, K.; Follen, M.; Aaron, J.; Pavlova, I.; Malpica, A.; Lotan, R.; and Richards-Kortum, R. 2003. Real-time vital optical imaging of precancer using anti-

epidermal growth factor receptor antibodies conjugated to gold nanoparticles. Cancer Res. 63: 1999-2004.

Song, K.C., Lee, S.M., Park, T.S. and Lee, B.S. 2009. Preparation of colloidal silver nanoparticles by chemical reduction method. Korean J. Chem. Eng. 26: 153-155.

Sumida, A.; Fukuen, S.; Yamamoto, I.; Matsuda, H.; Naohara, M.; and Azuma, J. 2000. Quantitative analysis of constitutive and inducible CYPs mRNA expression in the HepG2 cell line using reverse transcription-competitive PCR. Biochem. Biophys. Res. Commun. 267: 756-760.

Sun, X. P.; Zhang, Z. L.; Zhang, B. L.; Dong, X. D.; Dong, S. J.; and Wang, E. K. 2003. Preparation of gold nanoparticles protected with polyelectrolyte. Chin. Chem. Lett. 14: 866-869.

Swales K.; and Negishi, M. 2004. CAR, driving into the future. Mol. Endocrinol. 18: 1589-1598.

Tinel, M.; Elkahwaji, J.; Robin, M. A.; Fardel, N.; Descatoire, V.; Haouzi, D.; Berson, A.; and Pessayre, D. 1999. Interleukin-2 overexpresses *c-myc* and down-regulates Cytochrome P-450 in rat hepatocytes. J. Pharmacol. Exp. 289: 649-655.

Tournier, C.; Thomas, G.; Pierre, J.; Jacquemin, C.; Pierre, M.; and Sauniew, B. 1997. Mediation by arachidonic acid metabolites of the H₂O₂-induced stimulation of mitogen-activated protein kinases (extracellular-signal-regulated kinase and c-Jun NH₂-terminal kinase). Eur. J. Biochem. 244: 587-595.

- Trubetskoy, O.; Marks, B.; Zielinski, T.; Yueh, M.; and Raucy, J. 2004. A simultaneous assessment of CYP3A4 metabolism and induction in the DPX-2 cell line. AAPS J 7(1): E6-E13.
- Tsutsumi, M.; Lasker, J. M.; and Takahashi, T. 1993. *In-vivo* induction of hepatic P4502E1 by ethanol – role of increased enzyme-synthesis. Arch. Biochem. Biophys. 304: 209-218.
- Tully, D. B.; Collins, B. J.; Overstreet, J. D.; Smith, C. S.; Dinse, G. E.; Mumtaz, M. M.; and Chapin, R. E. 2000. Effects of arsenic, cadmium, chromium, and lead on gene expression regulated by a battery of 13 different promoters in recombinant HepG2 cells. Toxicol. Appl. Pharmacol. 168: 79-90.
- U.S. Food and Drug Administration. 2006. Drug interaction studies. Guidance for Industry. Rockville: Food and Drug Administration.
- Vakharia, D. D.; Liu, N.; Pause, R.; Fasco, M.; Bessette, E.; Zhang, Q.; Kaminsky, L. S. 2001. Effect of metals on polycyclic aromatic hydrocarbon induction of CYP1A1 and CYP 1A2 in human hepatocyte cultures. Toxicol. Appl. Pharmacol. 170: 93-103.
- Wang, Y.; Li, Y.; and Wang, B. 2007. Stochastic simulations of the cytochrome P450 catalytic cycle. J. Phys. Chem. B 111: 4251-4260.
- Westerink, W. M. A.; and Schoonen, W. G. E. J. 2007. Cytochrome P450 enzyme level in HepG2 cells and cryopreserved primary human hepatocytes and their induction in HepG2 cells. Toxicol. In Vitro 21: 1581-1591.
- Xu, J.; Yu, S.; Sun, A. Y.; and Sun, G. Y. 2003. Oxidant-mediated AA release from astrocytes involves cPLA₂ and iPLA₂. Free Radic. Biol. Med. 34: 1531-1543.

- Yonzon, C. R.; Zhang, X.; and Van Duyne, R. P. 2003. Localized surface plasmon resonance immunoassay and verification using surface-enhanced raman spectroscopy. P. Soc. Photo-opt. Ins. 5224: 78-85.
- You, C. C. M.; Miranda, O. R.; Gider, B.; Ghosh, S. P.; Kim, E.; Drdogan, B.; Krove, S. A.; Bunz, U. H. F.; and Rotello, V. M. 2007. Detection and identification of proteins using nanoparticles? Fluorescent polymer “chemical nose” sensors. Nat. Nanotechnol. 2: 318-323.
- Zhang, T.; Stilwell, J. L.; Gerion, D.; Ding, L.; Elboudwarej, O.; Cooke, P. A.; Gray, J. W.; Alivisatos, A. P.; and Chen, F. F. 2006. Cellular effect of high doses of silica-coated quantum dot profiled with high throughput gene expression analysis and high content cellomics measurements. Nano Lett. 6: 800-808.
- Zharov, V. P.; Kim, J. W.; Curiel, D. T.; and Everts, M. 2005. Self assembling nanoclusters in living systems: application for integrated photothermal nanodiagnosics and nanotherapy. Nanomedicine 1: 326-345.
- Zhou, J; Ralston, J.; Sedev, R.; and Beattie, D. A. 2009. Functionalized gold nanoparticles: synthesis, structure and colloid stability. J. Colloid Interface Sci. 331: 251-262.

APPENDICES

APPENDIX A

Characterization of AuCi and AuPEI

Table 4 UV absorption of citrate and PEI-stabilized AuNPs after preparation and 1 month storage

Citrate-stabilized AuNPs			
Condition	[Au] : [trisodium citrate]	Peak of UV absorption (nm)	
		After preparation	1 month storage
1	1 : 4	520	521
2	1 : 8	521	523
3	1 : 16	531	537
PEI-stabilized AuNPs			
Condition	[Au] : [PEI]	Peak of UV absorption (nm)	
		After preparation	1 month storage
1	1 : 0.35	513	514
2	1 : 0.7	514	516
3	1 : 1.4	522	524

APPENDIX B

Cytotoxicity test of AuNPs on HepG2

Table 5 Viability of HepG2 cells after incubated with AuCi for 48 h

Concentration of AuCi (μM)	Viability (%)	
	Average	SD ($n = 8$)
0.1	87.34	10.44
1	89.85	14.47
2	92.23	9.13
5	91.46	9.47
10	95.35	3.99
20	84.96	5.35
50	88.18	9.34
90	89.96	8.54

Table 6 Viability of HepG2 cells after incubated with AuPEI for 48 h

Concentration of AuPEI (μM)	Viability (%)	
	Average	SD ($n = 8$)
0.1	32.63	47.67
1	35.11	47.88
2	34.45	50.17
5	35.31	48.68
10	36.45	51.10
20	36.77	42.37
50	49.17	39.43
90	62.83	47.02

APPENDIX C

Fold induction of CYPs by AuNPs and inducers

Table 7 Fold induction of CYP genes in HepG2 cells after incubation with inducer or AuNPs (mean \pm S.D., $n = 4$)

Condition	Inducer ^a	AuCi 1 μ M	AuCi 10 μ M	AuPEI 0.1 μ M	AuPEI 1 μ M	DMSO
CYP1A1	3.30 \pm 0.82*	1.17 \pm 0.35	1.51 \pm 0.38	1.66 \pm 0.17*	1.68 \pm 0.35*	0.99 \pm 0.20
CYP1A2	8.08 \pm 2.41*	2.27 \pm 0.83	2.32 \pm 0.35*	2.59 \pm 1.00	2.08 \pm 0.56*	0.63 \pm 0.18
CYP2C9	3.00 \pm 1.20*	1.27 \pm 0.40	1.65 \pm 0.39*	0.77 \pm 0.24	1.11 \pm 0.48	0.70 \pm 0.22
CYP2E1	1.42 \pm 0.26*	1.12 \pm 0.36	1.17 \pm 0.45	1.69 \pm 0.27*	1.39 \pm 0.88	-
CYP3A4	2.90 \pm 0.91*	1.03 \pm 0.08	0.93 \pm 0.30	0.96 \pm 0.15	0.64 \pm 0.22	1.01 \pm 0.19

* Significantly different from an untreated control (= 1 fold), $p \leq 0.05$

^a α -Naphthoflavone (α NF) for CYP1A1 and CYP1A2; rifampicin (Rif) for CYP2C9 and CYP3A4; ethanol (EtOH) for CYP2E1

Table 8 Fold induction of CYP genes in HepG2 cells after incubation with a mixture of inducer and AuNPs (mean \pm S.D., $n = 4$)

Condition	Inducer^a	AuCi 1 μM + Inducer	AuCi 10 μM + Inducer	AuPEI 0.1 μM + Inducer	AuPEI 1 μM + Inducer
CYP1A1	3.30 \pm 0.82	1.40 \pm 0.34*	1.58 \pm 0.26*	1.56 \pm 0.54*	2.29 \pm 0.40
CYP1A2	8.08 \pm 2.41	5.89 \pm 0.49*	2.69 \pm 0.86*	7.46 \pm 0.96	12.70 \pm 1.12*
CYP2C9	3.00 \pm 1.20	0.76 \pm 0.14*	1.50 \pm 0.41*	1.50 \pm 0.52*	2.02 \pm 0.29
CYP2E1	1.42 \pm 0.26	0.78 \pm 0.04	0.94 \pm 0.32	0.88 \pm 0.29	0.72 \pm 0.13
CYP3A4	2.90 \pm 0.91	1.55 \pm 0.10*	2.28 \pm 0.24	1.61 \pm 0.60*	2.10 \pm 0.66

* Significantly different from an inducer, $p \leq 0.05$

^a α -Naphthoflavone (α NF) for CYP1A1 and CYP1A2; rifampicin (Rif) for CYP2C9 and CYP3A4; ethanol (EtOH) for CYP2E1

BIOGRAPHY

Miss Ladear Wangcharoenrung was born on January 20, 1984 in Bangkok, Thailand. She graduated with a Bachelor Degree of Pharmaceutical Sciences in 2006 from the Faculty of Pharmacy, Srinakharinwirot University, Thailand.

Publication:

Warisnoicharoen, W.; and Wangcharoenrung, L. 2009. Disorder of cytochrome P450 expression is inducible by gold nanoparticles? Biosci. Hypotheses 2: 184-185.